

SESSION 5

**FILTERS AND FILTRATION**

Monday: July 25, 1994  
Co-Chairmen: H. Gilbert  
R. G. Dorman

**HEPA FILTER CONCERNS - AN OVERVIEW**

J. F. Leonard

**A NOVEL PERMANENTLY MAGNETISED HIGH GRADIENT MAGNETIC  
FILTER USING ASSISTED CAPTURE FOR FINE PARTICLES**

J. H. P. Watson

**THE DEVELOPMENT OF A HEPA FILTER WITH IMPROVED DUST  
HOLDING CHARACTERISTICS**

J. Dymont, C. Hamblin

**EFFECT OF HUMIDITY ON THE FILTER PRESSURE DROP**

J. Vendel, P. Letourneau

**PRELIMINARY FIELD EVALUATION OF HIGH EFFICIENCY STEEL  
FILTERS**

W. Bergman, G. Larsen, R. Lopez, K. Wilson, K. Simon, L. Frye

**CLOSING COMMENTS OF SESSION CO-CHAIRMAN DORMAN**

# 23rd DOE/NRC NUCLEAR AIR CLEANING AND TREATMENT CONFERENCE

## HEPA FILTER CONCERNS - AN OVERVIEW

James F. Leonard  
U. S. Department of Energy  
Defense Programs, DP-31  
Washington D. C. 20585

### Abstract

The U. S. Department of Energy (DOE) recently initiated a complete review of the DOE High Efficiency Particulate Air (HEPA) Filter Program to identify areas for improvement. Although this process is currently ongoing, various issues and problems have already been identified for action that not only impacts the DOE HEPA filter program, but potentially the national and international air cleaning community as well.

This paper briefly reviews a few of those concerns that may be of interest, and discusses actions initiated by the DOE to address the associated issues and problems.

Issues discussed include: guidance standards, in-place testing, specifications, Test Facilities, portable units, vacuum cleaners, substitute aerosols, filter efficiencies, aging/shelf life/service life, fire suppression, handbook, Quality Products List (QPL), QA testing, and evaluations.

### I. Introduction

An overall review of HEPA filter materials, manufacturing techniques, uses, tests, research, and system designs, reveals that many improvements can be made in the HEPA filter arena.

In addition, problems with material quality, aging, filter failures, special applications, and lack of guidance, indicate that additional evaluations, research, and other actions are necessary to resolve a wide variety of issues and problems.

The DOE is currently evaluating its overall HEPA filter program and has identified numerous areas for improvement. A DOE HEPA Filter Working Group has been formed to look at the issues and advise management concerning resolutions and priorities.

Some of the concerns identified for resolution are included in this paper for information, including actions currently underway by the DOE.

## 23rd DOE/NRC NUCLEAR AIR CLEANING AND TREATMENT CONFERENCE

### II. HEPA Filter Issues

Aging: HEPA filters are fiberglass paper products that deteriorate (weaken) with age. The aging affects the ability of the HEPA filters to continue to meet normal and abnormal conditions.

No definitive guidance is available concerning Shelf Life or Service Life of HEPA Filters although we rely heavily on this safety component to protect workers, the public, and the environment.

In-place tests, delta pressure gauges, and visual inspections do not address the deteriorating structural strength issue.

Some HEPA filters in DOE facilities have been found to be reaching ages in excess of 30 years old. In addition, many filters are subjected to heat, pressure, moisture, and chemicals which can speed up the aging process. These older filters usually contain high quantities of hazardous materials. In some cases the filters contain non-radioactive materials or mixed hazardous materials.

Failure of the filters during normal and abnormal conditions can occur, particularly during accident conditions in which the facility is relying heavily on the ability of the filters.

A mini-study on HEPA filters using the DOE Occurrence Reporting and Processing System (ORPS) computer database, was performed to determine if there is evidence of filter problems. Results of the mini-study indicates that HEPA Filters are failing due to aging and other factors. Also, some separate, recent research into the issue revealed problems associated with the aging process. Enough information has been collected to suggest that additional research, evaluations, and testing is warranted.

The DOE is currently trying to determine if a time frame for replacing HEPA filters is reasonable and should be instituted. Additional research to help determine the scope of the problem is necessary.

Results of some recent research and limited testing by the DOE on aging is presented elsewhere in the conference papers.

Quality Products List (QPL) and Filter Testing: Testing of filters and filter materials for certification and inclusion on the QPL was previously conducted by the Department of Army, with some limited testing performed by the DOE. Based upon a letter from the Army dated March 16, 1994, the Army will maintain their

## 23rd DOE/NRC NUCLEAR AIR CLEANING AND TREATMENT CONFERENCE

testing facility but will no longer require testing for the QPL and will therefore no longer maintain the list.

Whether to test (and how much), or not test, needs to be revisited. Although the NRC and the DOE previously co-funded a QA/Acceptance pre-installation filter testing program, the NRC does not now require the commercial user to perform quality assurance and acceptance testing prior to installation of the filters. However, the DOE continues to perform filter acceptance and quality tests before installation, and currently maintains 3 Filter Test Facilities (FTFs) for this purpose.

Results of the FTF QA/Acceptance tests (which are different than in-place tests) indicate that the testing is not only desirable but necessary. The overall failure rate is approximately 3-4% with some models/manufacturers reaching 85-100% failures. The most common mode of failure is excessive penetration. The failure rate of respirator cartridges is approximately 1%.

Some non-DOE organizations make use of the DOE FTFs and pay to have their filters tested prior to installation.

The DOE has also discovered failed filters where the manufacturer did not have their products tested and included on the QPL.

In addition, some research and testing by the DOE into the cause of some recently failed new HEPA filters indicate that not all manufacturers are maintaining their products to the necessary material requirements. The new HEPA filters were structurally weak and prone to failure. In many cases the new filters failed the in-place test performed immediately after installation. This created the problem that the new, but now contaminated, filters had to be disposed of as radioactive waste while subjecting workers to unnecessary exposures while performing the extra installation and removal of the new filters (some filter changes are high potential contamination/radiation jobs). The failure of the HEPA filters to meet the required quality assurance tests, despite the requirements in the purchase orders, illustrates the need for DOE to conduct its own QA tests.

The results of research and testing on these failed filters is presented elsewhere in these conference papers.

The DOE currently maintains QPL testing capability at the Rocky Flats Filter Test Facility at Golden, Colorado but is not presently performing routine QPL-type testing. The DOE is currently reviewing filter testing needs in light of recent changes to the Army QPL program, and the DOE research on filter failures.

## 23rd DOE/NRC NUCLEAR AIR CLEANING AND TREATMENT CONFERENCE

Assumed Efficiencies of HEPA Filters During Accidents: There are no standards or definitive guidance concerning efficiencies of HEPA Filters during abnormal or accident conditions. The continued efficient operation of the filters under these conditions is important since many facilities rely heavily on the HEPA Filters to prevent exposure of radioactive materials to workers, the public, and the environment. However, facilities often do not consider or evaluate the effect of adverse conditions on the HEPA filters, and the resulting significantly reduced performance and efficiency.

During abnormal or accident conditions, HEPA filters could fail to perform their function of capturing hazardous materials, or, structurally fail releasing significant quantities of the hazardous materials they have accumulated (e.g. millions of curies of radioactive material or other hazardous substances).

The two items above on Aging and Quality Assurance Testing exemplify the real concerns of potential filter failures under adverse conditions.

The DOE is developing a standard to provide guidance concerning assumed efficiencies of HEPA Filters during abnormal and accident conditions. A draft of the standard has been completed and is starting through the DOE Standards Review Program. Information on the standard is presented elsewhere in these conference papers.

Nuclear Air Cleaning Handbook: The Nuclear Air Cleaning Handbook (ERDA 76-21), subtitled Design, Construction, and Testing of High Efficiency Air Cleaning Systems for Nuclear Applications, first issued in 1976 and used throughout the air cleaning community, needs updating to reflect latest technology improvements as well as changes in applicable codes and standards.

The Handbook, to promote development of safe, effective HEPA Filter systems, is currently undergoing revision by the DOE. Professor Mel First, at the Harvard University Air Cleaning Laboratory, is heading the revision effort.

Portable Air Cleaning Units and HEPA Vacuum Cleaners: Currently there are no standards that sufficiently cover special HEPA Filter applications such as the portable air cleaning units, radiological vacuum cleaners, and small in-line HEPA filters. Existing standards apply primarily to facilities.

Without specific direction and guidance, facilities are failing to properly test and use the filters. For example, some facilities run their portable HEPA units at twice the rated velocities of the HEPA Filters. This invalidates the certification of the filters and causes the filters to have an efficiency less than that required to qualify as a HEPA Filter. In addition it puts extra pressure on the filter structurally.

## 23rd DOE/NRC NUCLEAR AIR CLEANING AND TREATMENT CONFERENCE

Failure of these type filters ejects hazardous materials directly into the workplace or environment, usually without any means to detect that this is happening since portable units do not usually have the type of backup instrumentation used with permanent facility applications.

During fiscal year 1995, the DOE intends to develop a guidance standard for these type HEPA Filter applications. In the meantime, until the standard can be developed, temporary minimum guidance on these special applications has been included in Article 464 of the DOE Radiological Control Manual.

Fire Suppression Systems: Many large HEPA filter systems have water fire suppression systems installed inside the filter plenum. Moisture can have a detrimental effect on the fiberglass paper media weakening the filter structurally and speeding the aging process.

Fire systems are routinely tested with the water impacting the filters. In addition, full use of the fire suppression system could cause significant damage, leakage, and/or filter blow out causing release of hazardous materials. On the other hand, a fire could also release hazardous materials.

The DOE is currently looking at this issue relative to new materials and technology.

Substitute Aerosols: Di-Octyl Phthalate (DOP) continues to be used as the challenge aerosol for testing HEPA Filters, although questions exist concerning its potential health hazard to humans.

Information on DOP, as a potential carcinogen, has been issued by the DOE Office of Health in a Health Hazard Alert dated May 1994. The Alert says that the DOE "is evaluating to what extent the current use of DOP poses a health hazard within the DOE complex." The Alert further requests employers to limit exposure to employees, but does not prohibit use of DOP.

However, the EPA, in the Federal Register, Vol 58, No. 191, Tuesday, October 5, 1993, deleted di-n-octyl phthalate (DnOP) from the list of toxic chemicals under section 313 of the Emergency Planning and Community Right-to-Know Act of 1986 (EPCRA). Based upon the rationale used to justify the action, there appears to be a loosening of requirements concerning the phthalates.

Substitute aerosols are an alternative and in some cases DOE contractors are already using substitutes such as Emery 3004.

The DOE is currently evaluating the issue.

## 23rd DOE/NRC NUCLEAR AIR CLEANING AND TREATMENT CONFERENCE

HEPA Filter Specifications: The DOE has found that its facilities are not consistent in the use of HEPA Filter Specifications. For example, some facilities use out-of-date or otherwise incorrect specifications. This has resulted in problems at the facilities and at the filter manufacturers.

During visits to media and filter manufacturing plants over the last year, the manufacturers complained it is difficult to maintain a wide range of filter designs, materials, and certifications when the specifications vary among various organizations and facilities. For example, having such a wide range of filter materials tested and put on the Qualified Products List (QPL) is time consuming and costly.

The DOE is currently revising and revamping an internal standard on Specifications for HEPA Filters, and looking at newer materials that might provide greater structural strength and resistance to fire and heat. A draft of the standard has been completed and is about to be introduced into the DOE Standards program for review/issue.

In-Place Testing of HEPA Filters: The majority of DOE and non-DOE facilities (approximately 80% by some estimates) were built before the development of current applicable Standards for the design and in-place testing of HEPA Filters. Many of the facilities, with a wide assortment of designs, cannot meet the current standards and use a variety of self developed, non-consistent approaches.

An effort is underway within the DOE to develop a guidance document to provide for an improved, consistent, in-place testing program. Work on the in-place testing guidance document should be completed during FY95.

### III. Conclusion

The above discussion on HEPA filter issues covers only a few of the many areas that can be addressed to collectively improve the design, use, and testing of HEPA filters.

Examples of other topical areas include gel seals, metal filters, new materials, delta pressure meters, laser spectrometers, training, and use of scrim materials.

The intent of this overview is to illustrate that when all the HEPA filter issues are taken as a whole, the conclusion is easily reached that numerous areas exist for improvement of the HEPA filter program as a whole.

DISCUSSION

**PALMER:** You stated that DOE is revamping an internal standard on specifications for a HEPA filter. One of the problems with the old standard is that it was never formally issued as a compliance document. What efforts will DOE make to more formally issue this specification, more like an order to follow when you specify HEPA filters, instead of just handing it over as a kind of guidance document? That is my first question. My second is, will it address both portable HEPA filtration devices and stationary devices? A lot of the vacuum cleaners you talked about use small round filters instead of the standard square filters mentioned in the specifications.

**LEONARD:** Vacuum cleaners are what we call a special application. We have an item in one of our contracts to work on it over the next fiscal year. We recognize that it is different, and we will probably pick up the specifications on it as we work on the standard. It won't be in the specification standard we are working on right now. For the specification standard we are working on now, we will have everybody in the Department of Energy (and I know there are some of you outside the Department of Energy who are interested) take a look at it. We are trying to find something that will cover most of the applications. I don't think we can cover them all, but we can cover most of them. It is amazing, but manufacturers are still getting requests to build filters to the old standard that we were using back in the early 70s for asbestos filters.

**FIRST:** I acknowledge the deterioration of filters in long storage. Is there any work going on by any manufacturers or government agencies to define the deterioration mechanism? In other words, instead of wringing our hands that the filters are failing, is anybody trying to find out how to keep them from failing as they age?

**LEONARD:** The manufacturers we have talked to have said they have been looking at some new materials and they have some new ideas. It is a tough question. We have been trying to figure out how to determine what the maximum storage time should be but I don't think there is a way to determine it. We can come up with a number, and just put it out there, but I don't think that is a way to go because the variables are so many: heat, moisture, pressure, chemicals. You can just go on and on. Our concern is, how far should we go with this. You can't simply let them sit there forever. Eventually, they will fail on you. The mechanism to determine the failure is an in-place test that is performed annually, or at some other interval. How do you know when the filter is going to fail? We are also very concerned about the structural strength of the filter. It can pass the in-place test and still be about ready to fall apart. That is one of the things we are concerned about with the aging process. So, if you have an accident, and you are depending on old filters to perform according to the specifications it had when new, it is not going to happen.

**CROSBY:** As a follow up to Palmer's question, a Battelle engineer at Oak Ridge named Val Bouchard (615-220-2654) has, in fact, a complete set of specifications for testing both the HEPA filter in vacuum cleaners and negative pressure filtration units. He has also written a procurement specification.

**LEONARD:** I am aware of that. We have been working with these people on some of the tests



## 23rd DOE/NRC NUCLEAR AIR CLEANING AND TREATMENT CONFERENCE

and on other things we are doing. There are quite a few other issues but that is one of the facilities that has had problems with filters. They use a lot of HEPA filters, and they have a lot of old designs.

Let me leave you with this. I have come to the conclusion that HEPA filters are like small print. A man went to his attorney and said, "I am buying this house, but look at the small print, page after page of it. Should I read it all?" The attorney replies, "Well, technically you really should read all the small print, but I can give you the bottom line. The bottom line is this, you keep making your payments and there isn't anything in that small print that can hurt you. But if you stop making those payments, there isn't anything in that small print that can save you." And that seems like about where we are headed.

## 23rd DOE/NRC NUCLEAR AIR CLEANING AND TREATMENT CONFERENCE

### A Novel Permanently Magnetised High Gradient Magnetic filter using assisted capture for fine particles

Professor J.H.P. Watson  
Institute of Cryogenics  
University of Southampton  
Southampton SO17 1BJ  
England

#### Abstract

This paper describes the structure and properties of a novel permanently magnetised magnetic filter for fine friable radioactive material. Previously a filter was described and tested. This filter was designed so that the holes in the filter are left open as capture proceeds which means the pressure drop builds up only slowly. This filter is not suitable for friable composite particles which can be broken by mechanical forces. The structure of magnetic part of the second filter has been changed so as to strongly capture particles composed of fine particles weakly bound together which tend to break when captured. This uses a principle of assisted-capture in which coarse particles aid the capture of the fine fragments. The technique has the unfortunate consequence that the pressure drop across the filter rises faster as capture proceeds than the filter described previously. These filters have the following characteristics: (1) No external magnet is required. (2) No external power is required. (3) Small in size and portable. (4) Easily interchangeable. (5) Can be cleaned without demagnetising.

#### 1 Introduction

This paper describes a permanently magnetised magnetic filter which uses the principle of assisted-capture in order to capture and retain extremely fine particles of  $\text{PuO}_2$ , for example, generated in the processing of materials in the nuclear industry.

As described in a previous paper<sup>(1)</sup>, the basis of the use of such a filter in the nuclear industry relies on the fact that much of the radioactive material is paramagnetic and the permanently magnetised magnetic filters described in this paper have the same important features as those described previously<sup>(1)</sup>, namely: (1) No external magnet is required. (2) No external power is required. (3) Small in size and portable. (4) Easily interchangeable. (5) Can be cleaned without demagnetising. Two uses have been proposed for such a filter:

(A) As a cleanable pre-filter in front of an absolute filter in order to reduce the load on the absolute filter and thereby increase its useful life. This greatly reduces the absolute filter disposal cost. This filter can also be used in de-commissioning to capture the magnetic fume produced by cutting steel with a plasma torch.

(B) To improve housekeeping in a glove-box by preventing the spread of fine  $\text{PuO}_2$  through the box by constantly circulating the air or part of the air through the filter. By adopting this measure operator exposure could be reduced.

In the earlier paper<sup>(1)</sup> a different design for a permanently magnetised magnetic filter was presented. Experimental work with this filter was carried out at BNFL, Sellafield and in Mol, Belgium using Cr powder which is a good magnetic simulant for  $\text{PuO}_2$ . The extractive and retentive capability of this filter on Cr powder was found to be excellent down to a particle diameter of  $0.5 \mu\text{m}$  which was the limit of the measurements<sup>(1)</sup>. Subsequently, work was carried out on plutonium oxide at BNFL, Sellafield which revealed inadequacies in the filter design when treating real plutonium dioxide.

The magnetic filter consisted of a perforated sheet of Chromindur wound on a central tube and consisted of approximately 76 turns. The particles pass out of holes in the central tube and then pass through 76 layers. The Chromindur was magnetised parallel to axis of the tube and consequently parallel to the plane of the sheet. Under these conditions when particles are captured by the sheet, it has been demonstrated the particles are repelled from the holes in the Chromindur sheet and captured on the material between the holes<sup>(2)</sup>. This configuration is illustrated in Fig 1. This meant for a material such as chromium powder passing through the sheets under radial flow, as particles are captured, the holes remain open so that the pressure drop increases very slowly as material is captured by the

## 23rd DOE/NRC NUCLEAR AIR CLEANING AND TREATMENT CONFERENCE

filter. Ironically, this advantage of the design also carried a severe weakness when dealing with a friable material which can generate very fine particles. This property of the configuration which retains particles in the filter in such a way that the holes are left open, often considered very desirable in a filter, is the main reason why the fines generated by the friable plutonium oxide pass easily through these open holes without being retained. The evidence for this conclusion comes from a number of sources. Scanning electron microscopy shows the particles of  $\text{PuO}_2$  are composed of angular platelets arranged as rosettes around a nucleation centre. Ultrasonic agitation or other mechanical processes can be used to break up the agglomerates. Another observation was that the  $\text{PuO}_2$  agglomerates with other dust particles so there is a small amount of active particles together with non-active material. If this other dust is non-magnetic it could be a problem for the magnetic filter as the magnetic susceptibilities of the composite particles will be reduced. A number of these properties of  $\text{PuO}_2$  were observed by Moss, Hyatt and Schulte<sup>(3)</sup>.

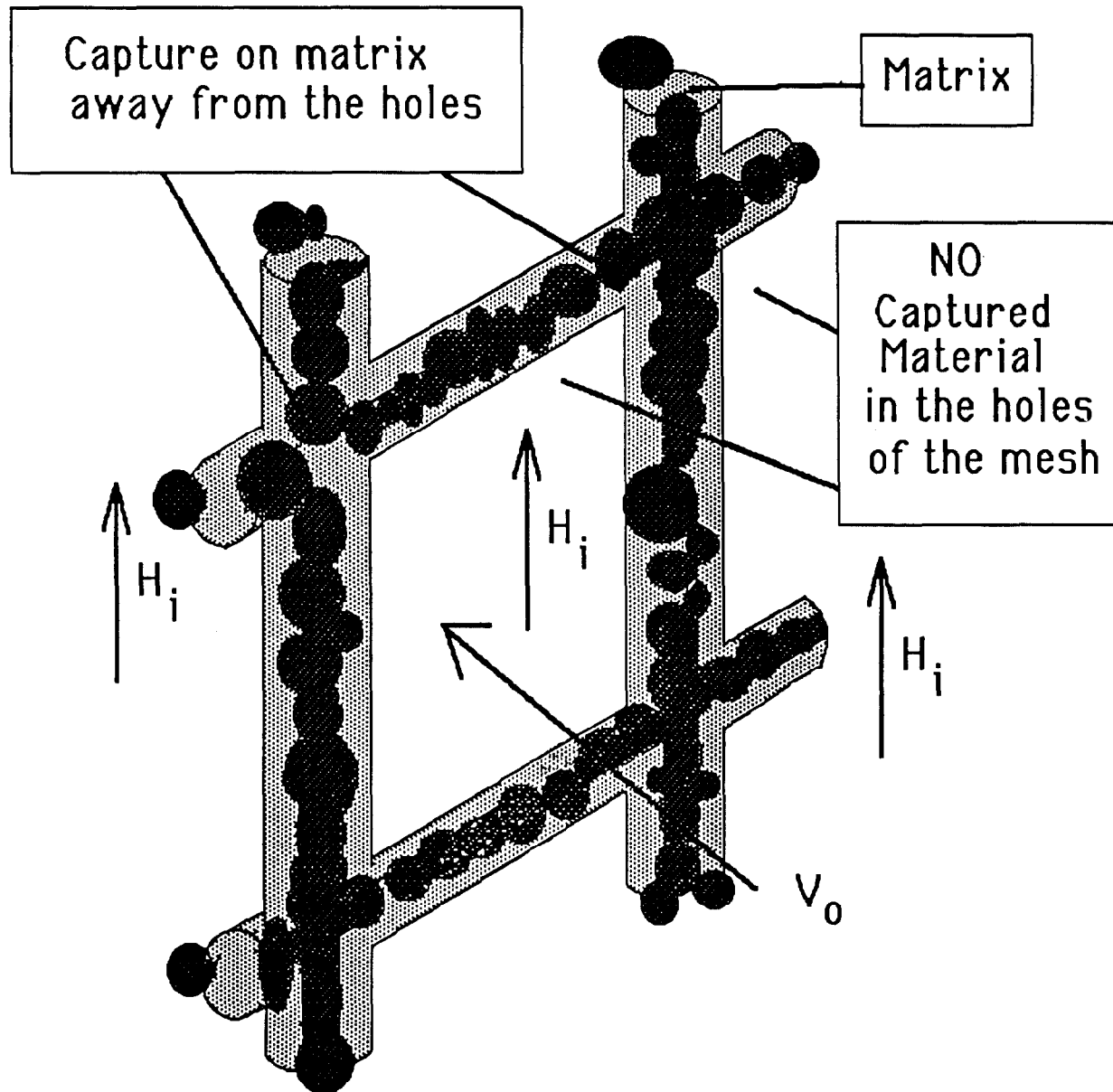


Fig 1 Shows a part of the permanently magnetised matrix. When the internal field  $H_i$  (demagnetising field) is in the plane of the mesh, no paramagnetic particles are captured in the holes. This means there is a small increase pressure drop as capture proceeds. The relatively coarse captured material is ineffectively placed in order to mechanically capture and entrain the fines which are lost.

The novel design presented here has a different configuration which should solve these problems for friable materials such as  $\text{PuO}_2$  and this is done by making the holes in the mesh attractive to magnetic particles. This occurs when the demagnetising field  $H_i$  is perpendicular to the plane of the mesh and in this part of the magnetisation curve, the magnetisation of the mesh is in the opposite direction to  $H_i$ . This configuration is illustrated in Fig 2. The relatively coarse particles now are captured within the holes. The captured particles are situated in a very good position to mechanically filter the fine particles from the flow. This means the fines are retained by the coarse particles captured within the holes and the retention is aided by the observed property of  $\text{PuO}_2$  to readily

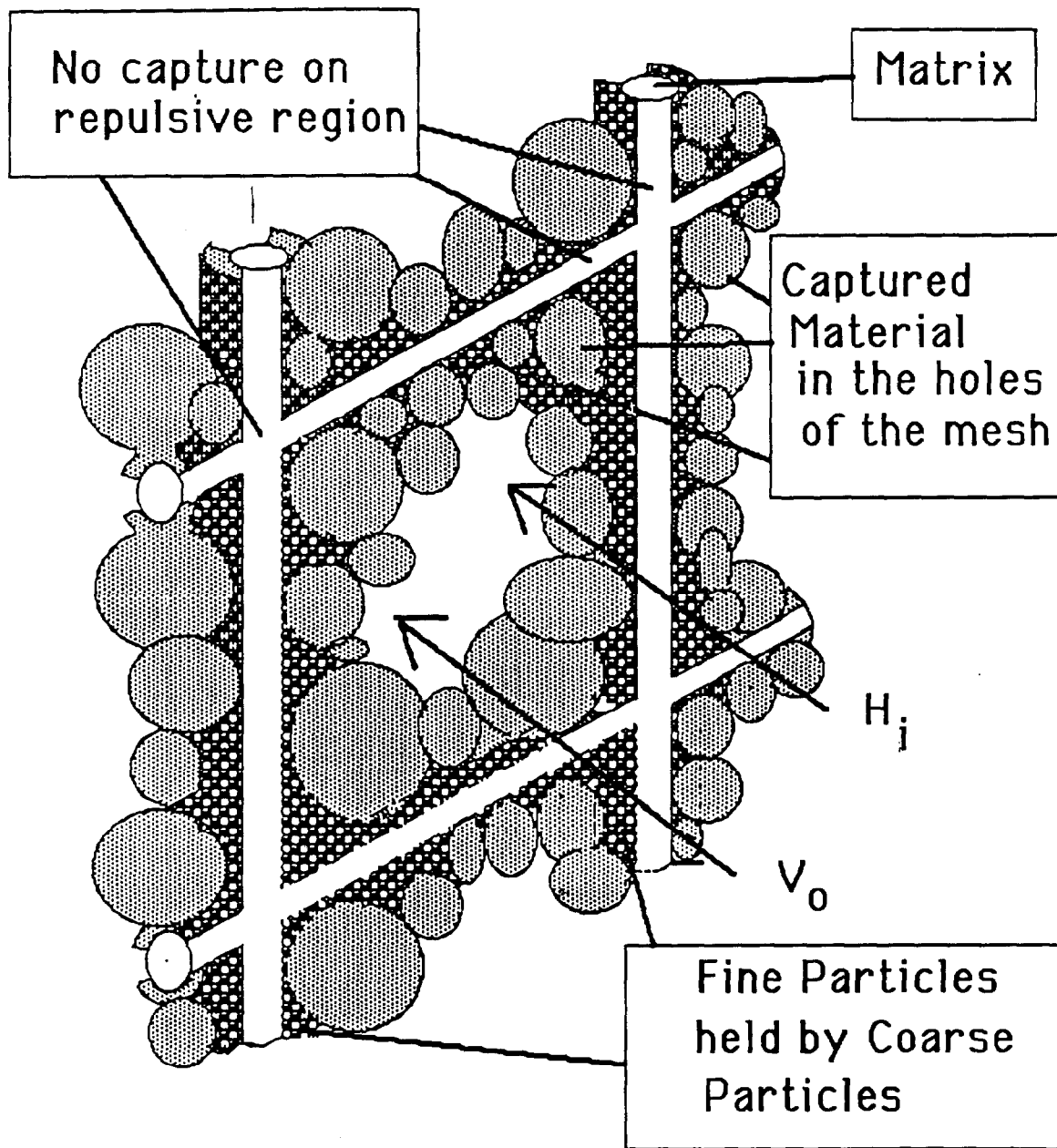


Fig 2 Shows part of the permanently magnetised matrix with the new configuration described in this paper. When the demagnetising field  $H_i$  is perpendicular to the plane of the mesh and in the portion of the magnetisation loop where the magnetisation of the mesh is in the opposite direction to  $H_i$ , as it is here, the matrix surface within the holes becomes attractive to paramagnetic particles. These particles are favorably placed to capture and retain fine particles by mechanical filtration and magnetic forces, as shown schematically here.

agglomerate <sup>(3)</sup> and by the magnetic forces.

Further, as the mesh is not rolled, the requirement for mechanical flexibility is not required for the mesh. It is therefore possible to use materials with much better magnetic properties than Chromindur. The more concrete choice of materials for the filter are discussed in section IV below. In the second section of the paper the theory of magnetic separation of monosize particles by permanently magnetised material is presented. In the third section the theory of **assisted capture** is discussed for the case where a wide range of particle size is present in the material to be filtered. The fourth section presents a new matrix configuration which will allow **assisted capture** to take place within the filter and which should considerably improve the performance of the filter.

II. Magnetic interaction of a particle and a magnetic wire

The theoretical model assumes a flow of paramagnetic particles carried by a fluid past a magnetised wire. We assume that the wire is ferromagnetic and hysteretic. The magnetic field in which the wire sits is the internal demagnetising field  $H_i$  of the whole assembly of hysteretic wires which have been magnetised to saturation after which the external applied field is reduced to zero. This leaves the residual demagnetising field as the magnetic field in which the wires and the paramagnetic particles sit. In this situation

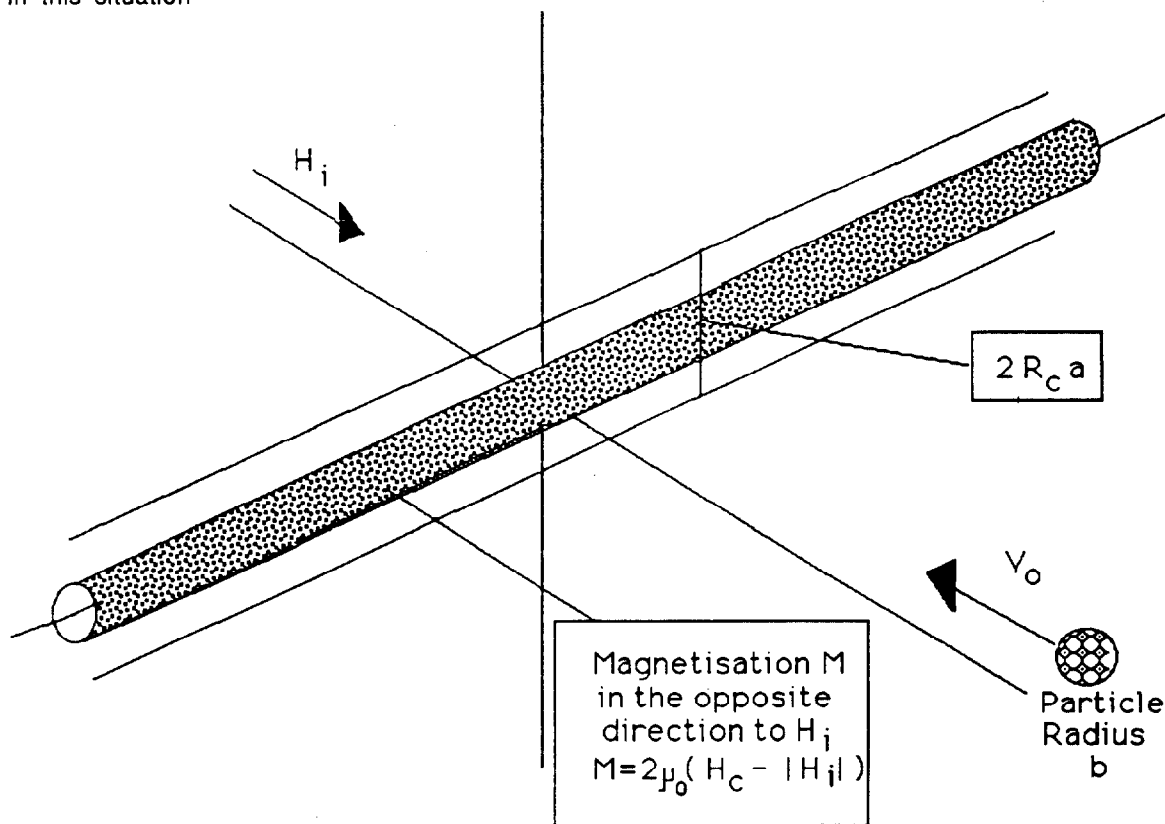


Fig 3 Shows the particle of radius  $b$  carried by a fluid of background velocity  $V_0$  moving parallel to the x-axis along which a magnetic field  $H_i$  is applied. It is necessary to determine the capture cross-section  $2R_c a$ , as shown.  $R_c$  is referred to as the capture radius.

the magnetisation  $M$  of the wire is in the opposite direction to the local magnetic field  $H_i$  and is given by  $M = 2\mu_0 (H_c - |H_i|)$  where  $H_c$  is the coercive force and  $\mu_0 = 4\pi (10^{-7})$  H/m, the permeability of free space. It is assumed that the wire is perpendicular in direction to this local field. From this following the methods by Watson<sup>(4)</sup> and more recently by Lawson, Simons and Treat<sup>(5)</sup> and Simons and Treat<sup>(6)</sup>, the equations of motion can be calculated and the capture cross-section  $2R_c a$  for the particle can be calculated. Here  $R_c$  is termed the capture radius and  $a$  is the wire radius. The geometrical significance of the capture cross-section is illustrated in Fig 3.

## 23rd DOE/NRC NUCLEAR AIR CLEANING AND TREATMENT CONFERENCE

The equations of motion determining the particle trajectories show and, in consequence, the capture of particles by a fibre, in a background magnetic field  $H_i$ , are determined by three parameters;

i)  $V_m/V_o$

where  $V_m$  is the 'magnetic velocity' containing all the important magnetic parameters in the system,

and  $V_o$  is the flow velocity.  $V_m$  is given by;

$$V_m = (2/9)\chi b^2 M|H_i|/\eta a \quad (1)$$

where  $\chi$  is the difference in susceptibility between the fluid of viscosity  $\eta$  and the particle of radius  $b$ .  $M$  is the magnetisation of the ferromagnetic wires of radius  $a$  and  $H_i$  is the local magnetic field, which for the case of the permanently magnetised matrix is referred to as the internal field  $H_i$ . Then using the expression given above for the wire magnetisation  $M$ , equation (1) becomes

$$V_m = (4/9)\chi b^2 \mu_o (H_c - |H_i|) |H_i|/\eta a \quad (1a)$$

$V_m$  is maximised with respect to  $H_i$  when  $|H_i| = H_c/2$ .

(ii) The short range parameter  $K$ , given by;

$$K = M/2\mu_o H_i = \{ H_c/|H_i| \} - 1 \quad (2)$$

If the wire is not magnetically saturated then  $K = 1$ . If  $V_m$  is maximised then  $K = 1$ , as the capture radius  $R_c$  depends on  $V_m/V_o$  and on  $K$ , the maximum in  $R_c$  does not necessarily occur at  $|H_i| = H_c/2$ .

iii) Stoke's number,  $N_{st}$ ;

$$N_{st} = (2/9)\rho_p b^2 V_o / \eta a = (Re/9)(\rho_p/\rho_L)(b^2/a^2) \quad (3)$$

$\rho_p$  and  $\rho_L$  are the particle density and the fluid density, respectively,  $Re$  is the wire Reynolds number where  $Re = 2 \rho_L V_o a / \eta$ . The efficiency of capture by the fibre can be adjusted by changing these parameters.

In the case of a permanently magnetised filter the optimisation of these parameters is crucial. To understand why this is so some background is necessary. In HGMS, weakly magnetic particles are captured by the combination of high fields and high field gradients. This is possible through the use of large electromagnets, or superconducting magnets so large values of  $V_m$  can be obtained. However there are some disadvantages which must be considered. One of these concerns the short range term,  $K$ , and the fact that for a soft ferromagnet with low hysteresis,  $K$  can only have a values between 0 and 1. In the case of a permanently magnetised filter the magnetic field is significantly smaller than that experienced in HGMS, however, because of magnetic hysteresis, it is possible to create values of  $K$  much greater than unity. Consequently, the optimisation of the field and magnetisation is crucially important. Given this optimisation, magnetic particles passing the filter elements will be captured if they are inside the capture radius  $R_c$  of that element.

The magnitude of  $R_c$  can be determined from  $V_m$ ,  $V_o$  and  $K$ . It is possible to build a model relating  $K$  to  $R_c$  for various  $V_m/V_o$  ratios. Fig 4 shows a graph of the capture radius as a function of the ratio of magnetic velocity to flow velocity. This graph has been obtained from data calculated by Watson<sup>(7)</sup>. These values were calculated for the case where dependence on the Stokes number is small and negligible.

It is interesting to look at the differences between conventional HGMS and HGMS with hysteretic materials. In conventional HGMS, the surface of the wire becomes divided into four regions, two of the regions are attractive to paramagnetic material and two repulsive to paramagnetic material. In hysteretic HGMS, the attractive regions become repulsive and vice versa. This has been discussed

## 23rd DOE/NRC NUCLEAR AIR CLEANING AND TREATMENT CONFERENCE

previously by Boorman, Watson and Bahaj<sup>(2)</sup>.

### III. Theory of Assisted Capture

#### III.1 Additional factors occurring in the magnetic separation of polydisperse systems

The theory discussed here has been presented in detail elsewhere<sup>(8)</sup>, however, because of the importance of the theory to the proposals made here, it appropriate to review the work in some detail.

Single-wire cells have been described by Watson & Rassi<sup>(9)</sup> and such cells have proved extremely useful in understanding the separation of many mineral systems. The particle trajectories and the magnetic build-up can be observed and recorded using a microscope, video camera and a video recorder. A video "frame grabber" in conjunction with a computing system has been used by Bahaj, Ellwood & Watson<sup>(10)</sup> to determine the magnetic properties of individual micron-sized particles from the particle trajectories near the wire. Watson and Li used a single-wire flow cell to investigate the

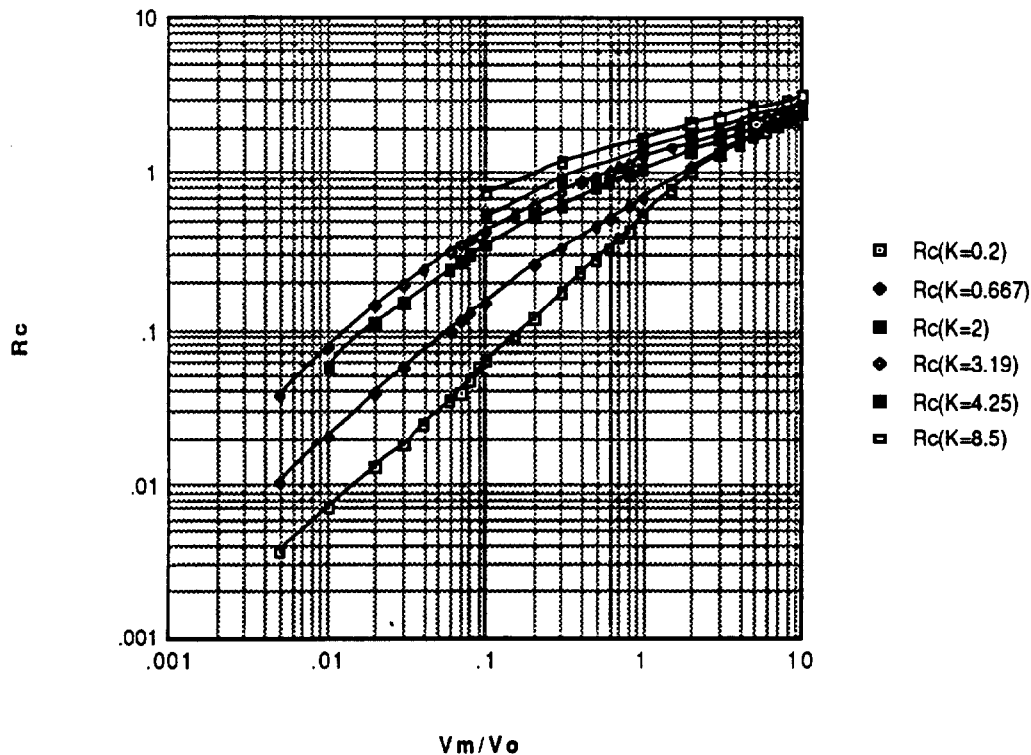


Fig 4 Shows  $R_c$  versus  $V_m/V_o$  for various values of the parameter  $K$ . For normal soft ferromagnetic material  $K$  can never be greater than 1, but for hysteretic material values of  $K \gg 1$  are possible.

capture of polydisperse particle systems onto a ferromagnetic wire magnetised by a uniform applied magnetic field. The novel feature of the cell used by Watson & Li<sup>(11)</sup> is that when the wire is loaded, the channel, containing the wire and the captured magnetic material, is frozen and the ice core containing the magnetic deposit can be removed for further detailed examination. With this technique Watson and Li<sup>(11)</sup> effectively demonstrated the occurrence of mechanical entrainment of non-magnetic material within the captured magnetics on the upstream side of the wire.

When particles collide with the surface of the magnetic deposit on the wire, they are acted on by a number of forces, such as, the viscous force due to the slurry flow which acts to drag the particles from the surface of the deposit, frictional and surface chemical forces which can hold the particles on

## 23rd DOE/NRC NUCLEAR AIR CLEANING AND TREATMENT CONFERENCE

the surface. In the operation of a separator normally the slurry would be optimally dispersed to minimise the adhesion between the different mineral species to improve selectivity but this is about the only general rule and in filtration problems, there would be considerable advantage to have the particles coagulate. Here the frictional term is of most interest. It was clearly observed by Watson and Li<sup>(11)</sup> means of the microscope system that when a slurry containing a mixture of paramagnetic and non-magnetic particles was passed through the flow cell with the field turned off few particles would deposit on the clean wire surface as the particles were easily swept away by the hydrodynamic force due to the slurry flow. It was observed however the magnetic deposit is rough on a scale of the deposited particle radius, as shown in Fig 5. If particles of smaller radius are present, they are able to penetrate into the deposit and be trapped there. If the particles are of radius less than half of that of the primary magnetic deposit, the the hydrodynamic drag on the particle will be greatly reduced and the probability of retention greatly increased. A model developed in section III.2 which includes some of the complicating factors of the filtration of a polydisperse particle distribution, that is a wide particle size distribution, in which mechanical trapping is included. This is attempted with a bimodal distribution in which all the particles have the same susceptibility.

In the simple force balance model of magnetic capture<sup>(12,13)</sup> the fluid drag on a magnetic particle in relation to the magnetic forces is such that  $V_m/V_o < 0.62$ , the particle can not be retained. The quantity  $f$  is ratio of the volume of material captured to the volume of the wire and the maximum value taken by  $f$  is  $f_{max}$  which depends on  $V_m/V_o$ . The factor  $f$  can increase until the azimuthal magnetic force is less than the azimuthal fluid drag force and this condition determines  $f_{max}$  so that when  $V_m/V_o = 0.62$  then  $f_{max} = 0$  (12,13).

$$f_{max} = (1/\pi)(V_m/V_o)^{2/3} \int_{3\pi/4}^{\pi} |1 - \cos\theta|^{2/3} d\theta - 1/4 \quad (4)$$

Effects of mechanical entrainment can be examined with this model. The particle size for the bimodal distribution is chosen so that for the small particles  $V_m/V_o < 0.62$  which means they are normally swept off the wire as  $f_{max} = 0$ . However, the large particles have  $V_m/V_o \gg 0.62$  and consequently any fine particles which are captured must be entrained mechanically. This therefore one of the simplest system which enable the consequences of mechanical entrainment to be considered. This model can easily be extended to the case where the magnetic susceptibilities of the two sizes are different as the appropriate parameter characterising the particles in  $V_m/V_o$  is  $\chi b^2$ . To extend the model to the case where  $V_m/V_o > 0.62$  for all the particles is more complicated and is not considered here.

This model gives very different results from the simple application of monodisperse theory to each particle size; the reasons for this are two-fold. First, mechanical entrainment was not included and second, that the capture radius  $R_{c0}$ , for a bare wire, is modified when capture proceeds, that is when  $f > 0$ , by multiplying  $R_c$  by a function  $G(f)$  where  $G(f) = 1/(1 + 4f)$ <sup>(13)</sup>,  $R_c = R_{c0}G(f)$  and contributions to  $f$  occur from all particle sizes which have been captured. The method of adding contributions from each particle size only gives the correct answer when  $f=0$  and  $G(0)=1$ .

The results are also extremely interesting for filtration problems when  $V_m/V_o \gg 1$  for the large particles while maintaining  $V_m/V_o < 0.62$  for the small particles and when it is desired to filter all the particles from the stream. The results are completely at variance with the conclusions arrived at using the method of adding contributions from each particle size. However, the model shows how a bimodal distribution can be optimally filtered which has important implications for the filtration of polydisperse systems.

### III.2 The magnetic separation of a paramagnetic bimodal distribution of particles with equal values of magnetic susceptibility

Now we can consider a bimodal particle distribution where the particles have radii  $b$  and  $B$  where  $B \gg b$  and  $V_o$  is chosen so that  $V_m(B)/V_o \gg 0.62$  and  $V_m(b) < 0.62$ . If the small particles impinge upon the bare wire, they will be swept off as  $V_m/V_o < 0.62$ , but the large particles will be able to form a 2-dimensional layer over the part of the surface of the wire surface which is attractive to paramagnetic.



## 23rd DOE/NRC NUCLEAR AIR CLEANING AND TREATMENT CONFERENCE

particles. If the small particles of radius  $b \ll B$  can pack between the large ones. These particles will not feel the full drag as determined in the Force-Balance model and therefore they can be retained with the holes and pockets in the surface of the deposited  $B$  particles which the studies with the single. This is shown schematically in Fig 5. If it is assumed that the particles are spherical, then in each layer the space between the large particles  $B$  which can accommodate the small particles  $b$  is a volume  $(4\pi/3)(\beta_{eB}-1)B^3$ , where  $\beta_{eB}$  is the packing factor for the particles  $B$ . The packing factor is obtained from the total volume of the deposit  $V_D$  as follows:

$$\beta_{eB} = V_D / n_p (4\pi/3) B^3 \quad (5)$$

where  $n_p$  is the number of particles in the deposit. If we assume only the top half is accessible to the small particles  $b$ , the volume available in which the small particles can be retained for every large particle captured is  $(2\pi/3)(\beta_{eB}-1)B^3$ . In the calculations which follow it is assumed that the packing is not very dense so that each large particle that is captured provides a volume of  $2B^3(2-\pi/3)$  in which small particles can be retained. From this assumption  $\beta_{eB} = 6/\pi = 1.91$ . For these small particles the probability of retention is identical to their capture probability which is not zero when  $f > f_{\max}(b)$  because when the particles  $b$  are retained between the particles  $B$  then the hydrodynamic drag is greatly reduced so that  $f_{\max}$  is determined by the large particles  $B$  as  $f_{\max}(B)$ . If the number of small particles captured is greater than the volume available to them which provided by the incoming large particles, the excess are small particles return to the slurry. Stating this more precisely, if

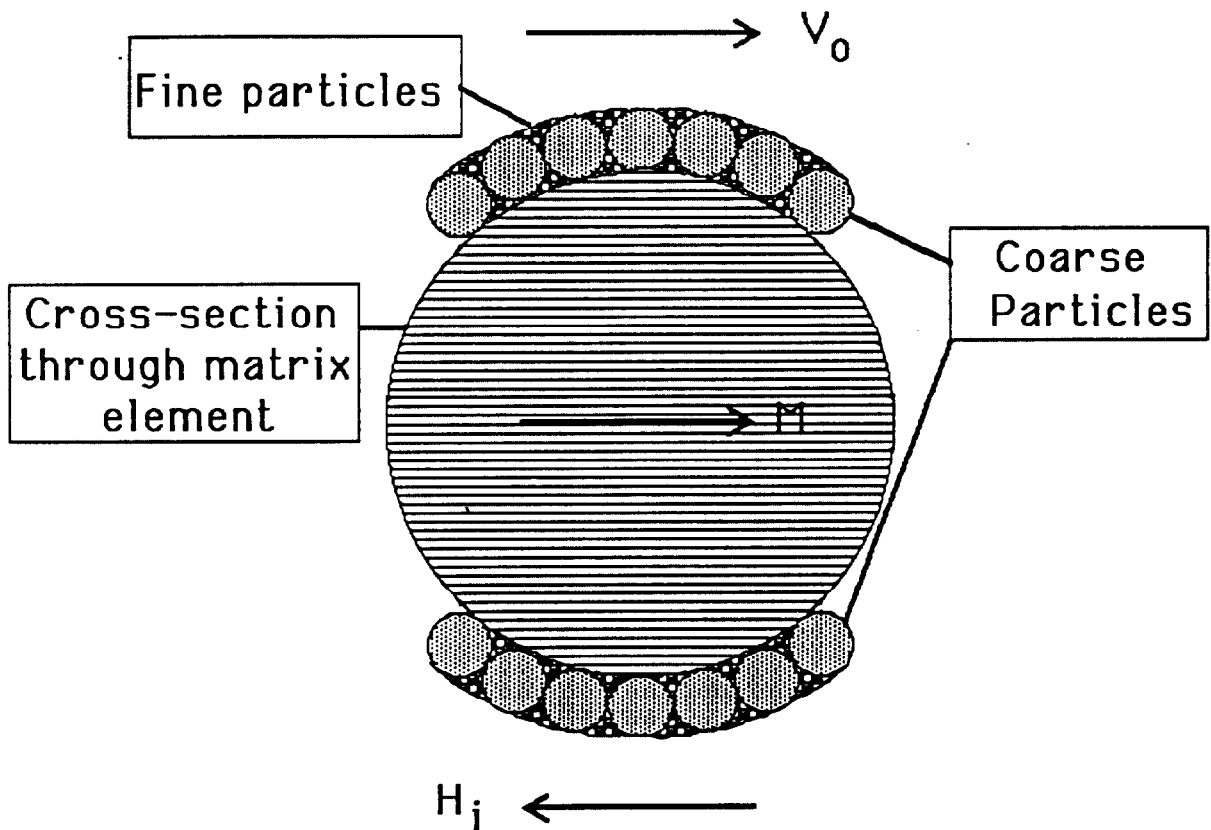


Fig. 5 Cross-section through the wire showing captured particles of radius  $B$  space shaded is occupied by particles of radius  $b$  wire .

$$dN_b(x)/dt < (\beta_{eB}/2\beta_{eb})(B/b)^3 dN_B(x)/dt \quad (6)$$

## 23rd DOE/NRC NUCLEAR AIR CLEANING AND TREATMENT CONFERENCE

where  $\beta_{eb}$  is the packing factor of the small particles into the volume provided by the large particles.  $N_b(x)$  and  $N_B(x)$  are the number of captured particles at position  $x/m^3$  of the matrix, for  $b$  and  $B$  respectively.

If  $dN_b(x)/dt$ , as determined by the separator equation with  $R_c(b)$  (13) given by  $R_c(b) = (V_m/2V_o)(1/(4f+1))$  satisfies the inequality (6), as the space provided by the large particles  $B$  is occupied by the small particles therefore the value of  $f$  is completely determined by the large particles  $B$ . This simplifies the equations, as  $f=f(B)$  and  $f(b)=f(B)$  and therefore  $R_c(b) = (V_m(b)/2V_o)(1/(4f(B)+1))$ , for the small particles  $b$ , and for the large particles  $R_c(B) = (V_m(B)/2V_o)(1/(4f(B)+1))$ . Combining these expressions for  $R_c(b)$  and for  $R_c(B)$  with the separator equation gives:

$$(dN_B(x)/dt)/(dN_b(x)/dt) = (R_B(x)R_{c_o}(B))/(R_b(x)R_{c_o}(b)) \quad (7)$$

This equation only applies when the particles  $b$  do not fill all the space provided by the captured  $B$  particles.

If the inequality expressed in (6) is not satisfied, then  $dN_b(x)/dt$  is given by

$dN_b(x)/dt = (\beta_{eB}/2\beta_{eb})(B/b)^3 dN_B(x)/dt$  and then excess particles  $b$ , arriving at the wire, are not retained and remain in the slurry. This expression for  $dN_b(x)/dt$  together with equation (8) determines the ratio  $R_b(x)/(R_B(x))$  at which the space provided by  $B$  is just filled and is given by

$$R_b(x)/(R_B(x)) = (R_{c_o}(B))/(R_{c_o}(b)) / ((\beta_{eB}/2\beta_{eb})(B/b)^3) \quad (8)$$

If  $B=2b$  then  $R_{c_o}(B)/R_{c_o}(b)=4$  and if  $\beta_{eB}=\beta_{eb}$  then equation (8) gives  $R_b(x)/(R_B(x))=1$ .

The behaviour of the separator can now be investigated within this model by solving the separator equations with the appropriate boundary conditions. Here the boundary conditions used correspond to usual operating practice in magnetic separation, namely

$$\begin{aligned} R_B(x,0) = N_B(x,0) = R_b(x,0) = N_b(x,0) = 0 & \quad L \geq x \geq 0 \\ R_B(0,\tau) = R_B(0), R_b(0,\tau) = R_b(0) & \quad (9a) \\ R_B(x,\tau) = R_b(x,\tau) = 0 & \quad \text{for } \tau < \epsilon_0 x/V_o \end{aligned}$$

These conditions correspond to the separator containing no particles initially and the flux of particles at the entrance remains constant in time until, after some time  $t_f$ , the required volume of particles have been fed and then the flux of particles is set to zero. This boundary condition is as follows:

$$R_B(x,\tau) = N_B(x,\tau) = R_b(x,\tau) = N_b(x,\tau) = 0 \quad \text{for } L \geq x \geq 0 \text{ and for } \tau > t_f \quad (9b)$$

We wish now to consider the capture of a bimodal system by the separator under boundary conditions outlined in equations (9a) and (9b). To illustrate the solution of this model, the following conditions were applied. The matrix occupied 5% of a cylindrical space that was 0.03 m in length with a cross-sectional area of  $1m^2$ . The applied field was 3 Tesla with a velocity of  $1ms^{-1}$ . The large particles have radius of  $10 \mu m$  and the fine particles a radius of  $4 \mu m$  and  $\gamma$ , the ratio of the volumes of coarse to fine is  $\gamma=1$ . The magnetic velocity of the coarse particles  $V_m(B)=1.804$  and for the fine particles  $V_m(b)=0.289$ . After the total volume of material applied to the separator, normalised to the volume of the matrix  $\alpha = 0.08$ , the concentration of  $N_B(x)$ , the concentration of the coarse particles  $B$ , and  $N_b(x)$ , the concentration of the fine particles  $b$ , as a function of position within the matrix is shown in Fig 6.

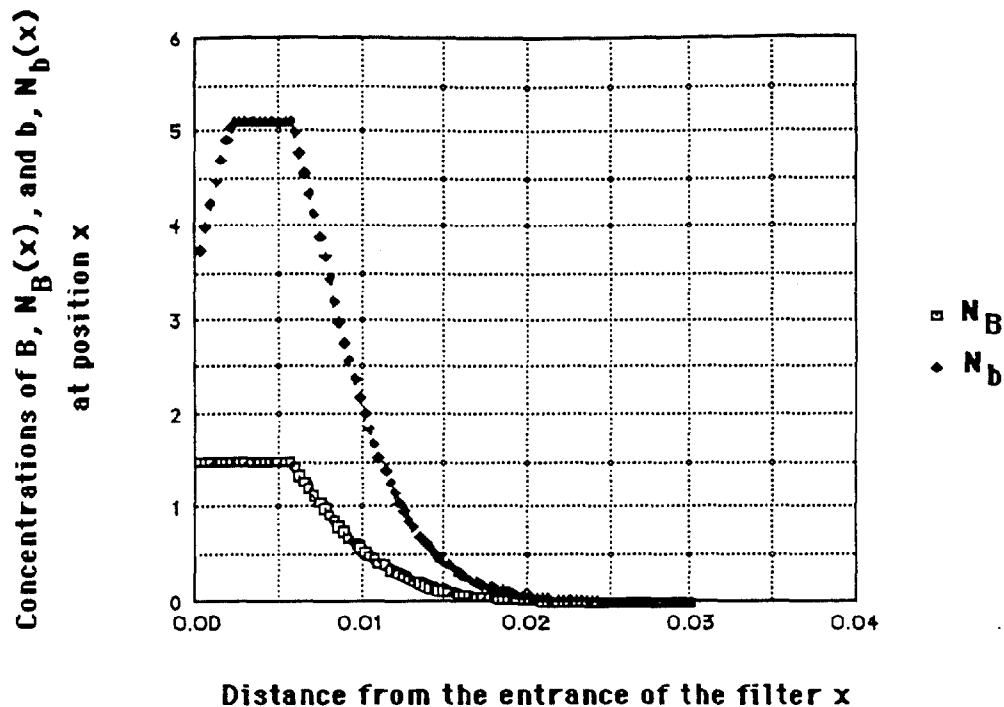


Fig 6  $N_B(x)$  and  $N_b(x)$  the (number of particles). $10^{-12}$  per unit volume of the coarse and the fine particles, respectively, in the separator at position  $X$  where  $X$  is the distance from the entrance of the separator. The magnetic velocities for the coarse and fine particles are 1.804 and 0.289 respectively. The volume of the particles fed to the filter divided by the volume of the matrix  $\alpha = 0.08$ .  $\gamma$ , the ratio by volume of coarse to fine particles, is  $\gamma = 1$ .

The fraction of the fine particles transmitted through the separator is 0.781 if the coarse particles were not present then all the fines would be transmitted. All the coarse particles are retained within the separator. The flow rate used in the calculations was 1 m/s and the concentration was 0.04% by volume and the total volume of slurry passed was  $0.3m^3$ . The distribution of particles captured within the separator is substantially the same as for a more concentrated slurry of smaller volume provided that  $\alpha$ , the total volume of the particles divided by the volume of the matrix and  $\gamma$ , the ratio by volume of coarse to fine particles, are held constant.

There are a number of features of interest in Fig 6, namely the concentration of the coarse particles in the separator  $N_B(x)$  is initially constant with  $x$  and at the maximum value given by equation (8) of  $N_B(x)=1.49(10^{12})/m^3$  with the fine particles  $b$  starting at  $x=0$  with a concentration of  $N_b(x)=3.76(10^{12})/m^3$ , corresponding to a fraction of 0.672 of the total space provided within the coarse particle buildup which can be calculated from equation(4). The relative of buildup of the coarse and fine particles is determined by equation(7), the capture rate at  $x=0$ , is initially greater for the large particles  $B$ , but for greater values of  $x$ , the capture of the fine particles  $b$  increases with  $x$  until  $(R_B(x)R_{CO}(B))/(R_b(x)R_{CO}(b))=1$  which, by equation (7) means that  $dN_B(x)/dt)/(dN_b(x)/dt)=1$ . This point is reached at  $x=0.002$  after which the concentration of the large particles  $B$  is  $N_B(x)=1.49(10^{12})/m^3$  and the fine particles  $b$  with a concentration of  $N_b(x)=5.10^9(10^{12})/m^3$  which corresponds to a fraction 0.921 of the total space available to the fine particles  $b$ . Beyond  $x=0.006$ , the flux of coarse particles  $B$  has dropped so low that the separator is not filled to the maximum value possible and in consequence the number the fine particles begin to fill the total volume available to them but which decreases rapidly with  $x$ .

It is interesting to consider the transmission of the fine particles  $b$  as the total volume of the particles applied to the separator is increased, that is, as  $\alpha$  is increased.

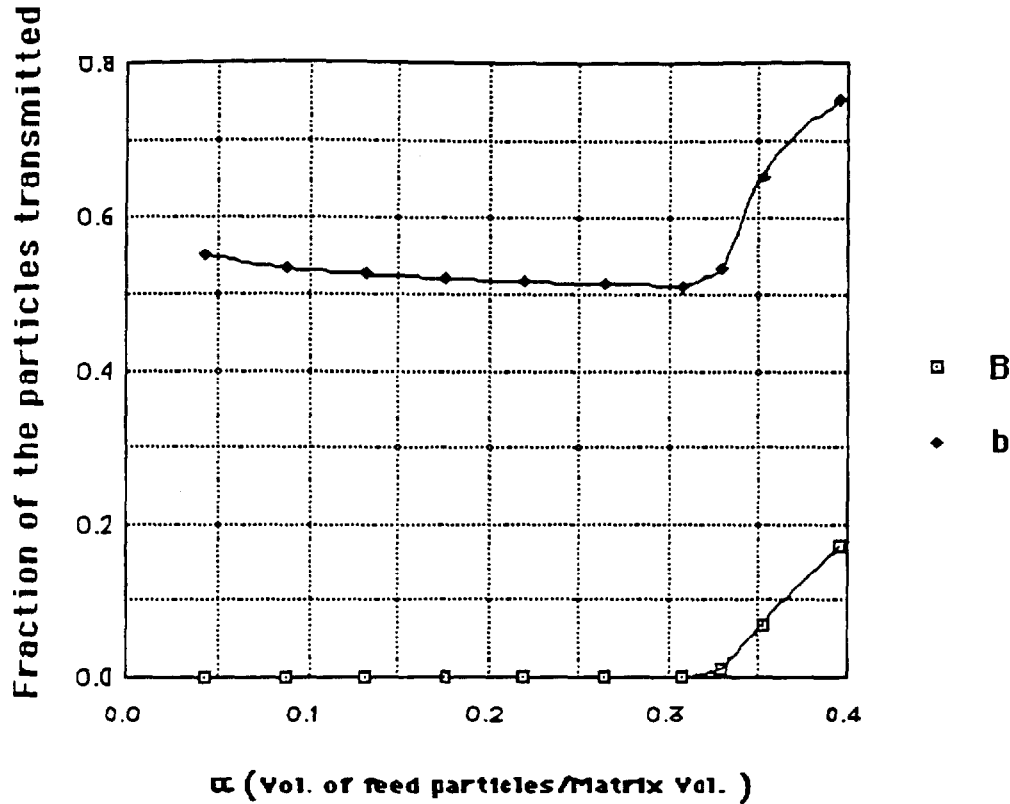


Fig 7 The fraction of the particles transmitted versus a ratio of the volume of the particles fed to the separator to the volume of the matrix for the coarse particles B and the fine particles b. The ratio of the volumes of coarse particles to fine particles  $\gamma$  is  $\gamma = 10$ . The length of the separator is 0.1 m. All the fine particles b would be transmitted in the absence of the coarse particles.

As shown in Fig 7, there is a small decrease in the fraction of fine particles b transmitted as the value of  $\alpha$ , the ratio of the volume of the particles fed to the separator to the volume of the matrix, is increased until breakthrough of the coarse particles B occurs when  $\alpha = \alpha_{max} = 0.3$  which is the maximum efficiency for the filtration of the fine particles. If it is assumed that no coarse particles escape before complete breakthrough then  $\alpha_{max} = f_{max}FL = N_B L$  where F is the fraction of the space in the filter occupied by the matrix and L is the length.

In the conventional treatment of magnetic separation for monosize particles, the number of particles leaving the separator decreases exponentially with the separator length L, it is interesting to consider the effect of length L on the transmission of fine particles in this assisted capture model. This can be done by examining the transmission of fine particles using the same ratio  $\gamma$  of coarse particles to fine particles of  $\gamma = 10$ , for a number of constant values of  $\alpha$ , versus the separator length L. As shown in Fig 8 the fraction particles transmitted is almost independent of the length L, except when the coarse particles are beginning to breakthrough at high values of  $\alpha$ . This is the type of behaviour expected for the coarse particles in the absence of an interaction with the fine particles, but in this case the transmission of the fine particles would be complete.

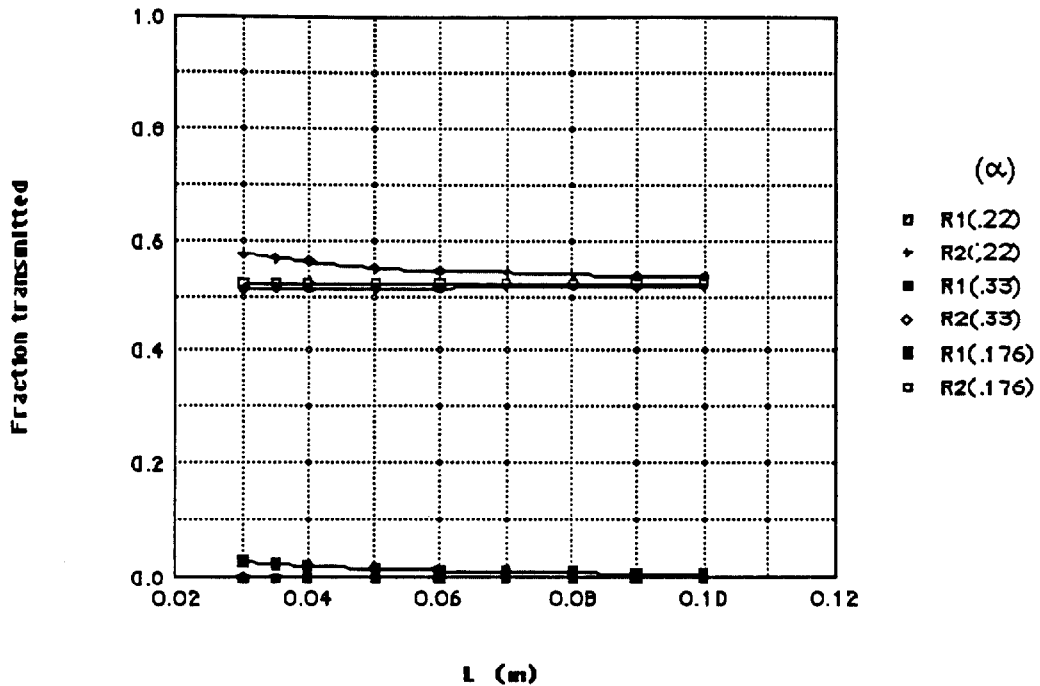


Fig 8 The fraction of particles transmitted through separators of various length  $L$  when the ratio of the volume of the particles in the feed to the volume of the matrix  $\alpha$  is used as a parameter. The curves for the coarse particles are near zero but the values for the fine particles are near 0.5. The ratio of the volumes of coarse to fine particles  $\gamma$  is  $\gamma = 10$ .

We can now consider reducing the number of fine particles transmitted, that is, we are attempting to filter out the fine particles by adjusting  $\gamma$  the volume ratio of coarse particles to fine particles. From Fig 8 it is known that the fraction of particles transmitted is almost independent of the length of the separator  $L$  if  $\alpha \ll \alpha_{max}$ . In the results of the calculations shown in Fig 9, the amount of the small particles  $b$  in each feed batch is held constant and this is fed mixed with various amounts of the coarse particles  $B$  so that  $\gamma$  reaches  $\gamma = 10$  (so that every point on the curve represents a separate experiment. This sequence is repeated for various applied magnetic fields. Fig 9 reveals that provided the coarse particles  $B$  do not breakthrough, the number of fine particles extracted depends almost entirely on  $\gamma$ , the ratio of the coarse particles to the fine particles. There is a weak dependence of number of small particles  $b$  retained in the separator on the applied magnetic field and, contrary to expectation from monodisperse theory, the number retained decreases slightly as the field increases.

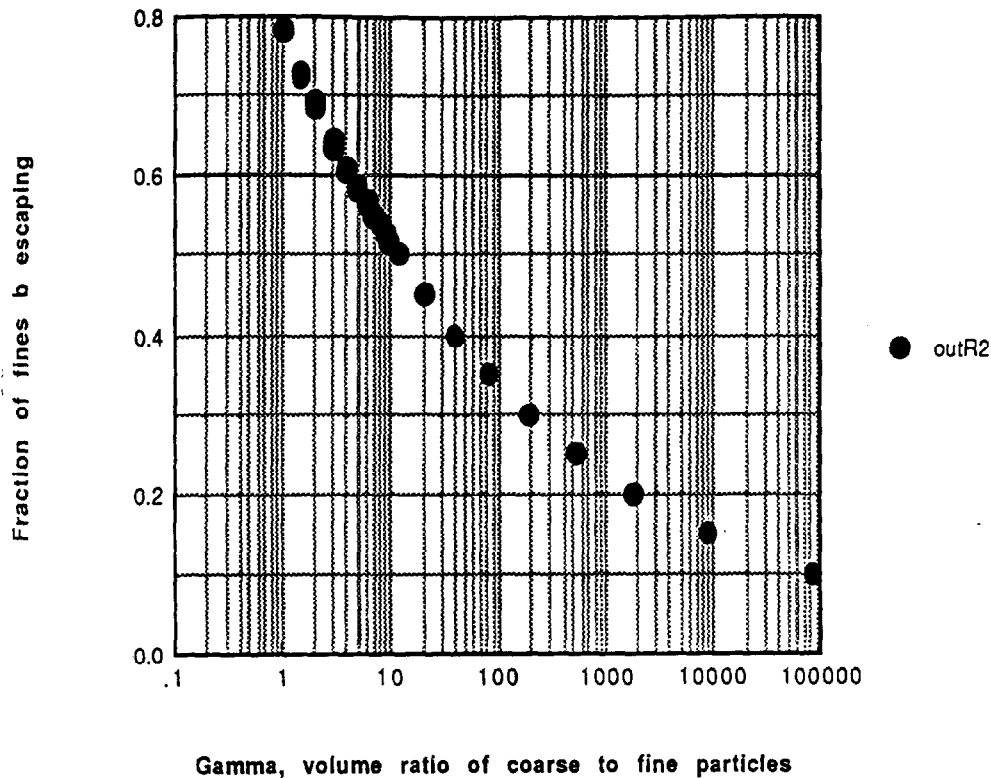


Fig 9 The fraction of small particles, radius  $b$ , transmitted through the separator versus  $\gamma$ , the volume ratio of coarse particles radius  $B$  to fine particles radius  $b$ . This conditional upon the the coarse particles not having filled the filter.

Summary of the effects produced on the filtration of fine particles

The result of assisted capture on the filtration and retention of the fines  $b$  can be summarised by saying the minimum transmission of  $b$  is achieved, for a particular filter, when the quantity of large particles  $B$  is just sufficient to achieve breakthrough. The fraction of  $b$  transmitted decreases as  $\gamma$ , the ratio of coarse particles  $B$  to fine particles  $b$ , increases but subject to the condition that breakthrough of  $B$  does not occur. High magnetic fields and long filters can therefore be used to decrease the transmission of the fine particles  $b$  by ensuring that breakthrough of  $B$  only occurs at smaller and smaller ratios of  $b$  to  $B$ , that is at large and larger values of  $\gamma$ .

IV. New design for the Permanently magnetised separator

Introduction

The development of this model requires an understanding of the filtration applications envisaged for the system. A filter is proposed consisting of a stack of expanded ferromagnetic metal mesh. The previous filter was made from a rbl of Chromindur, as described in an earlier paper<sup>(1)</sup>. The mesh was an hysteretic ferromagnetic, but it had the important property of is also flexibility with a low but usable coercive force of 300 Oersted. Chromindur is a product of Telcon Metals Ltd, Crawley, England. The new filter geometry as shown in Fig 10a does not require the property of flexibility so other materials, particularly those developed for the recording industry with their high values of coercivity, can be used.

Magnetic Materials for use in the filter

Basically there are two choices for materials, namely: Thin film materials and particulate materials of various types<sup>(14)</sup>. Most of the films available have the residual magnetisation in the plane of the film which is not useful for the filter structure described here. The reason for this is the shape anisotropy energy of a thin sheet magnetised perpendicular to the sheet. To stabilise the magnetisation perpendicular to the sheet, additional anisotropy must be introduced. This can be done in Co films by introducing Cr to a level of near 20 at. %<sup>(15)</sup>. At these compositions values of the coercivity of  $H_c = 65 - 105 \text{ kAm}^{-1}$  can be achieved.

A better choice for a matrix material are metal particles, a material which again originates in the magnetic recording industry and in that industry has allowed high coercive forces to be achieved. For example, with pure iron particles, which are available commercially, values of coercivity are typically  $H_c = 91.5 \text{ kAm}^{-1}$ . Pure iron particles are very reactive and must be passivated by exposing them to a mixture of  $N_2$  and  $O_2$ . The final product is an acicular particle surrounded by a coating of  $Fe_2O_3$  and  $Fe_3O_4$ . The stability of iron particles has been studied by Lee, Hu & Madudid<sup>(17)</sup>

Performance of the filter with a material composed of passivated iron particles

The matrix was magnetised perpendicular to the surface of the sheets in the stack; the sheets being perpendicular to the flow of the suspension and also parallel to the filter axis. The applied field was then reduced to zero, and, due to the hysteretic nature of the material, the filter remained magnetised with an internal field strength  $H_i$  of  $21.8 \text{ kAm}^{-1}$ . This determined from the dimensional ratio  $L/D = 1/3$  having a demagnetising factor of  $N_z = 0.52$ . The magnetisation of the unit cell can be approximated by assuming that it is due to the strands perpendicular to  $H_i$  but in the opposite direction to it. Under these conditions the magnetisation of the strands is largely determined by the demagnetisation factor of the strand, approximately 2, and the coercivity of the material assumed to be  $91.5 \text{ kAm}^{-1}$ .

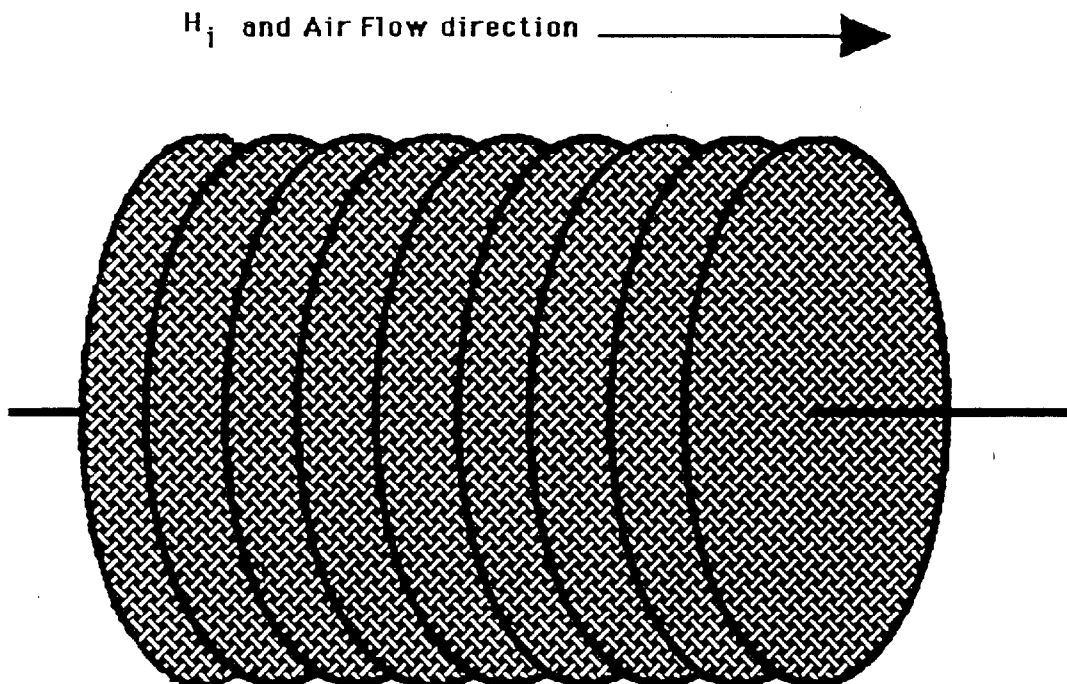


Fig 10a Structure of the prototype filter shows a few of the 124 sheets of circular cross-section in the form of a mesh stacked in a cylindrical tube made from a recording material composed of passivated iron particles. The sheets of material composing the filter are perpendicular to the flow. The unit cell is the repeated unit generating the two-dimensional sheet. The separation of the sheets is 0.2 mm

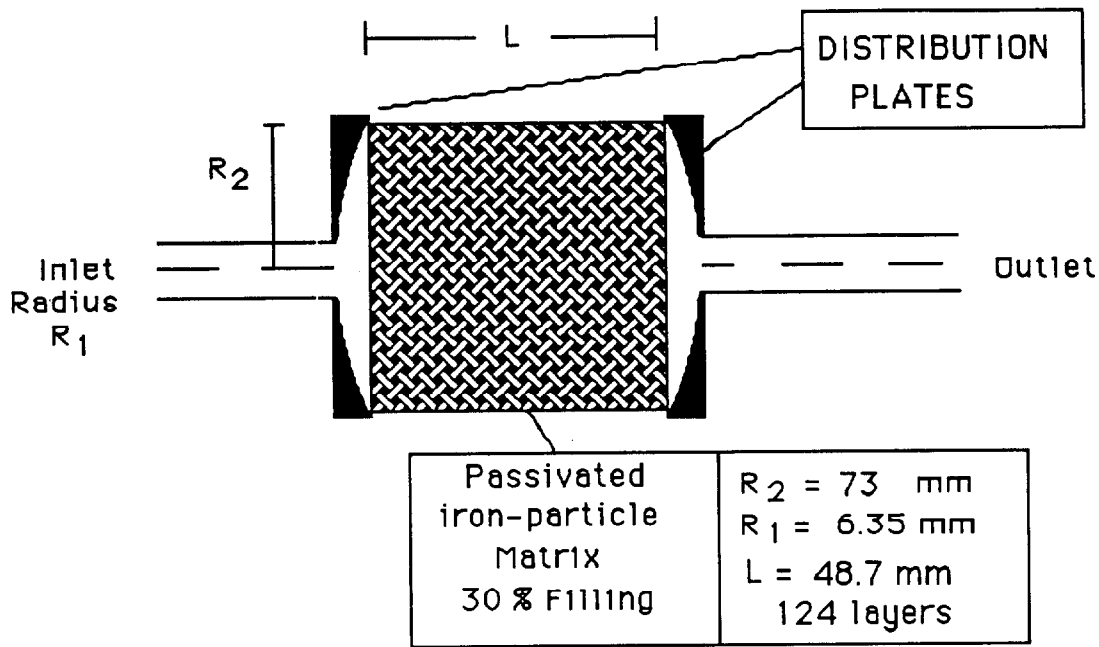


Fig 10b Shows a section parallel to and passing through the axis of the cylindrical filter. The gas flow is parallel to the cylindrical axis. The cross-section perpendicular to the flow is circular is proposed that  $L = 48.7 \text{ mm}$ . The separation between the layers is  $0.2 \text{ mm}$  and the thickness of the sheet is  $0.2 \text{ mm}$ . The material is magnetised perpendicular to the plane of the sheets that is parallel to the axis of symmetry. The distribution plates are designed to equalise the Bernoulli pressures.

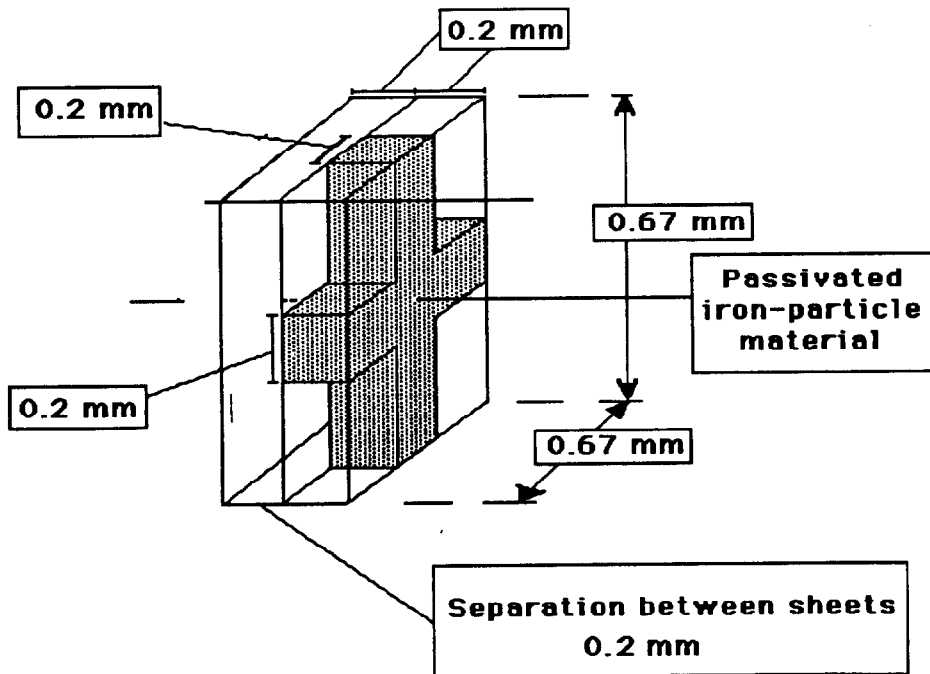


Fig 11 The unit cell of the structure is shown. The sheets of chromindur  $0.2 \text{ mm}$  thick are separated from each other by  $0.2 \text{ mm}$  and are generated by displacements of  $6.7 \text{ mm}$  parallel to the directions  $6.7 \text{ mm}$  shown. The stack is generated by displacements in the perpendicular direction.



## 23rd DOE/NRC NUCLEAR AIR CLEANING AND TREATMENT CONFERENCE

Consequently, with the magnetisation of the wires  $M_W$  given by  $M_W = 2(H_C + H_i)$ , and  $H_i$  has the value  $H_i = 21.8 \text{ kAm}^{-1}$ . The magnetisation  $M_W$  of those legs perpendicular to the field, on which most magnetic capture will occur due to the large field gradients, is therefore  $M_W = 139.5 \text{ kAm}^{-1}$ . The magnetic velocity  $V_m$ , given in equation (1a), can now be evaluated. For fibres of radius,  $a = 0.1 \text{ mm}$ , and particles of radius,  $b = 0.5 \text{ microns}$ , with a susceptibility of  $5 \times 10^{-5}$  (S.I. units), the resulting magnetic velocity  $0.038 \text{ mm/sec}$ . In this case a value of  $V_m/V_0 = 0.03$  would be suitable, i.e. a flow velocity of  $1.25 \text{ mm/sec}$ . The corresponding value of  $K$ , given in equation (2), is  $3.19$  and the value of  $R_C$  versus  $V_m/V_0$  for  $K=3.19$  is plotted in Fig 4. If we assume that the particles are captured on the legs of the matrix with the value of the capture radius shown in Fig 4, the effective cross-section per unit area,  $\#_1$ , for the first sheet is given by( using the dimensions shown in Fig 11 is  $\#_1 = 0.204R_C$ , therefore the fraction transmitted is  $1 - \#_1 = 1 - 0.204R_C$ . The number of particles captured in the next sheet was obtained for the if the second sheet by determining the extra cross-section provided by the second sheet when the second sheet is shifted parallel to the plane of the sheet from perfect registration with the first sheet. Assuming that all shifts have equal probability, the extra cross-section provided by the second sheet can be averaged. The fraction transmitted by the second sheet is therefore  $1 - \#_2 = 1.33 R_C^2 (1 - 0.3R_C)^2$ . The next 123 sheets are all similar the total number of particles escaping is given by  $(1 - \#_1)(1 - \#_2)^{123}$ . These expressions have been evaluated and are shown in Fig 12 for the case where the matrix is clean for a number of particle sizes.

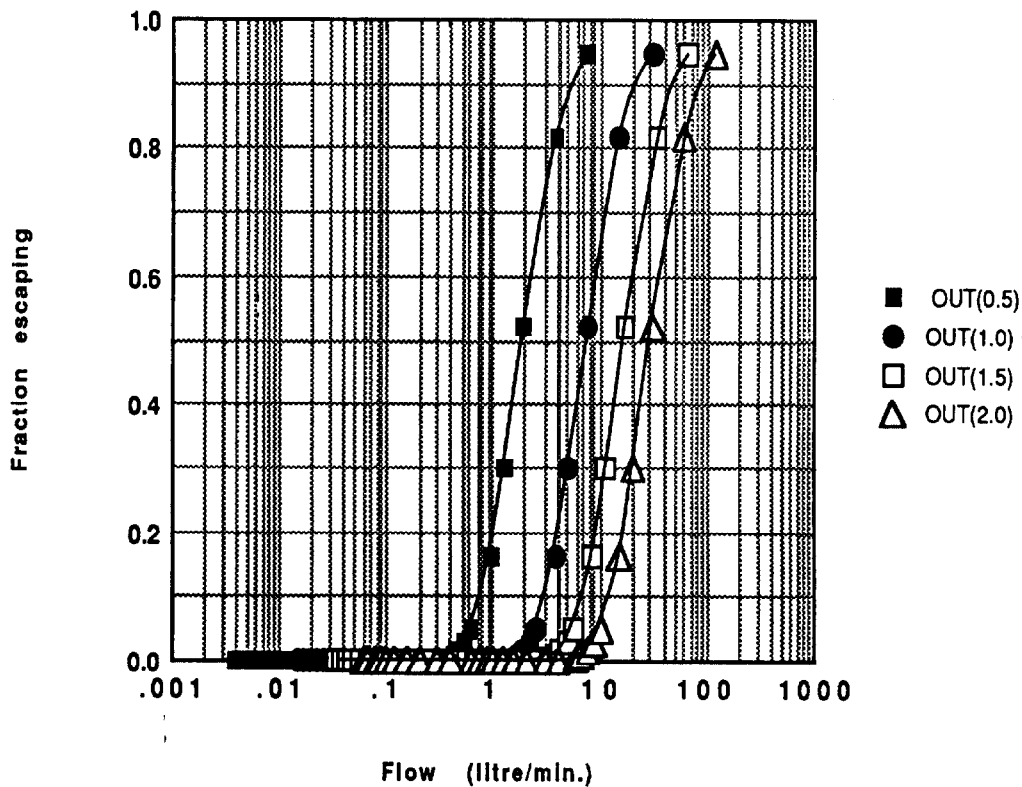


Fig 11 Shows the expected initial performance of the new filter orientation when it is clean.

## 23rd DOE/NRC NUCLEAR AIR CLEANING AND TREATMENT CONFERENCE

Assuming a 30% filling factor, the total volume of the matrix is  $2.4 \times 10^{-4} \text{ m}^3$ . As already mentioned, the mass loading envisaged in the flow to the filter is about  $0.04\text{gm}/\text{m}^3$ . Nasset and Finch<sup>(16)</sup> introduced a quantity called the loading number which has been modified to incorporate interparticle frictional forces and this loading number has been used to calculate the total mass that can be theoretically captured by the filter. Using this approximation the total mass captured by the filter has been calculated to be 485 grams. If the mass loading in the gas to the filter is  $0.04\text{gm}/\text{m}^3$ , and assuming a 30% packing factor for the material built up on the wires, this means the total processed volume will be  $12,125 \text{ m}^3$ , and, at a flow rate of  $0.036 \text{ m}^3/\text{hr}$  the overall lifetime of the filter will be 38 year. It should be realised that this is a small prototype filter. Practical filters will need to process somewhere in the region of  $10 \text{ m}^3/\text{hr}$  if they are to be useful.

The performance of the filter which is expected in the presence of assisted capture is shown in Fig 11.

### VI. References

- (1). J.H.P. Watson, and C.H. Boorman, A Permanently Magnetised High Gradient Magnetic Filter for Glove-box cleaning and increasing HEPA life, 21st DOE/NRC Nuclear Air Cleaning Conference, Ed. M.W. First. 2 vols. (San Diego, California, U.S.A.: U.S. Nuclear Regulatory Commission, 1990) 2: 762-771.
- (2). C.H. Boorman, J.H.P. Watson, and A.S. Bahaj, "Magnetic Filtration Studies using a permanently Magnetised matrix," IEEE Trans. Magn. MAG-23.No. 5, September (1987): 2755 - 2759.
- (3). W.D. Moss, H.C. Hyatt, and H.F. Schulte, "Particle size studies on plutonium aerosols," Health Physics 5 (1961): 212-218.
- (4). J.H.P. Watson, "Magnetic Filtration," J.Appl.Phys. 44. No. 9, September (1973): 4209 - 4213.
- (5). William F. Lawson, William H. Simons, and Richard P. Treat, "The dynamics of a particle attracted by a magnetized wire," J.Appl. Phys. 48.No. 8, August (1977): 3213-3224.
- (6). William H. Simons, and Richard P. Treat, "Particle trajectories in a lattice of parallel magnetized fibers," J.Appl. Phys. 51.(1), January (1980): 578-588.
- (7). J.H.P. Watson, High-Capacity, High-Intensity Magnetic Separators using Low Magnetic Field, Sixth International Conference on Magnet Technology, MT-6., Ed. M. Polák, J. Kovacovsky, L. Krempasky and S. Takáč. 2 vols. (Bratislava, Czechoslovakia: ALFA, Bratislava, Czechoslovakia, 1977) 1: 308 -314.
- (8). J.H.P. Watson, "Selectivity and Mechanical retention in the magnetic separation of polydisperse, mixed mineral systems - Part 1," Minerals Engineering 7.Nos. 5/6 (1994): 769-791.
- (9). J.H.P. Watson, and D. Rassi, Single-wire Magnetic Separation: A Diagnostic Tool for Mineral Processing, MINTEK 50-International Conference on Mineral Science and Technology, Ed. L.F. Haughton. 2 vols. (Sandton, South Africa: The Council for Mineral Technology, Randburg, South Africa, 1984) 1: 335 - 340.
- (10).A.S. Bahaj, J.H.P. Watson, and D.C. Ellwood, "Determination of Magnetic susceptibility of loaded microorganisms in Bio-magnetic Separation.," IEEE Trans. Magn. MAG-25.No. 5, September (1989): 3809-3811.
- (11). J.H.P. Watson, and Z. Li, "A study of mechanical entrapment in HGMS and vibration HGMS," Minerals Engineering 4.Nos. 7-11 (1991): 815-823.
- (12). Y.A. Liu, and M.J. Oak, "Studies in Magnetochemical Engineering Part 2: Theoretical Development of a Practical Model for High-Gradient Magnetic Separation," AIChE Journal 29.No 5, September (1983): 771 - 779.
- (13). J.H.P. Watson, "High Gradient Magnetic Separation-Solid-Liquid Separation," Solid-Liquid Separation, Ed. Ladislav Svarovsky 3rd ed. (London: Butterworth & Co (Publishers) Ltd., 1989)
- (14). G. Bate, "Magnetic Storage Media," Concise Encyclopedia of Magnetic & Superconducting Materials, Ed. Jan Evetts 1 vols. (Oxford, England: Pergamon Press, 1992) 1: 245-253.
- (15). T.C. Arnoldussen, "Thin Film Recording Media," Proc. IEEE 74.No. 11 (1986): 1526-1539.
- (16). J.E. Nasset, and J.A. Finch, "A static model of high gradient magnetic separation based on forces within the fluid boundary layer," Industrial Applications of Magnetic Separation, Ed. Y.A. Liu 1 vols. (New York, N.Y., USA: Institute of Electrical and Electronic Engineers, 1979) 1: 188-196.
- (17). T-H. D. Lee, S. Hu & N. Madudid IEEE Trans. Magn 25 4374-89(1987).

DISCUSSION

**WREN:** Does the required magnetic field depend on the susceptibility of the particles? If so, how will the required field be predetermined when the susceptibility would change due to the change in the particle composition with time? Would the deposited particles affect the localized field? If so, what is the effect of that?

**WATSON:** For ordinary paramagnetic materials the changes in the magnetic field as build-up proceeds are small and can be neglected. If the materials were ferromagnetic they would affect local fields and would increase capture.

THE DEVELOPMENT OF A HEPA FILTER WITH  
IMPROVED DUST HOLDING CHARACTERISTICS

J Dymont<sup>(1)</sup> and C Hamblin<sup>(2)</sup>

(1) AWE Aldermaston, (2) UKAEA Harwell

Abstract

A limitation of the HEPA filters used in the extract of nuclear facilities is their relatively low capacity for captured dust. The costs associated with the disposal of a typical filter means that there are clear incentives to extend filter life. The work described in this report are the initial stages in the development of a filter which incorporates a medium which enhances its dust holding capacity.

Experimental equipment was installed to enable the dust loading characteristics of candidate media to be compared with those of the glass fibre based papers currently used in filter construction. These tests involved challenging representative samples of the media with an air stream containing a controlled concentration of thermally generated sodium chloride particles. The dust loading characteristics of the media were then compared in terms of the rate of increase in pressure differential. A number of "graded density" papers were subsequently identified which appeared to offer significant improvements in dust holding.

In the second phase of the programme deep-pleat filters ( $1,700 \text{ m}^3\text{h}^{-1}$ ) incorporating graded density papers were manufactured and tested. Improvements of up to 50 % were observed in their capacity for the sub-micron sodium chloride test dust. Smaller differences (15 %) were measured when a coarser, carbon black, challenge was used. This is attributed to the differences in the particles sizes of the two dusts.

1. Introduction

The high efficiency particulate air (HEPA) filters used in the United Kingdom nuclear industry are purchased against specifications<sup>(1)</sup>. These documents detail the requirements for the materials of construction and the basic design, and prescribe general performance criteria. The increasing financial and technical implications of radioactive waste treatment, storage and disposal has heightened interest in the dust holding capacity of HEPA filters. In order to maintain compatibility with existing plant any increase in dust holding must be achieved without increasing the overall dimensions of current filter designs, or with detriment to operating parameters.

Previous workers have investigated and compared the dust holding capacity of various HEPA filter designs<sup>(2)</sup>. However, these studies did not specifically measure the performance of the filtration medium employed or the effects of different media in identical filters. It is possible therefore that a filter constructed with a medium possessing favourable dust loading characteristics could achieve longer life.

This report describes a method of rapidly testing the dust loading characteristics of small samples of candidate filtration media with a thermally generated sub-micron test aerosol. This procedure identified the potential advantages offered by a range of "graded density" papers developed by Whatman International Ltd. Results are also presented which show that improvements in dust loading are also evident for  $1,700 \text{ m}^3\text{h}^{-1}$  deep-pleat filters constructed with the most promising examples of these media.

### 2. Experimental Programme

The experimental programme was conducted in two phases. Initial experiments sought to establish the dust loading properties and the basic performance characteristics of a number of filtration media.

The second phase involved the manufacture and testing of conventional deep-pleat HEPA filters which incorporated the most promising of the media identified.

#### 2.1 Media Testing and Selection.

The strength properties and particle collection efficiency of the candidate materials were assessed for compliance with the current filter media specification<sup>(3)</sup>. A significant number of the media available (especially those manufactured from non-glass fibres) are at least an order of magnitude thicker than the glass fibre based papers currently used in HEPA filters. These materials were not included in the test programme due the practical difficulties of incorporating sufficient medium into existing filter size envelopes.

The dust loading characteristics of the samples of filter medium were investigated using the equipment shown in Figure 1. A test aerosol was generated by feeding a stick of sodium chloride into an oxy-propane flame to produce particles with a mass median diameter (mmd) of  $0.20 \mu\text{m}$  and a geometric standard deviation of 1.4. The salt particles were then injected into the primary duct (250 mm ID) to become thoroughly mixed with the main system air flow. The flow rate within the primary duct was monitored by a standard orifice plate and controlled by adjusting speed of the fan.

The provision of a rectangular HEPA filter, to protect the fan, allowed the air to be discharged back into the laboratory area.

A secondary (test) flow was extracted from the primary duct and passed through an 80 mm diameter disc of filter medium mounted 20 duct diameters downstream of the abstraction point. Flow within the test duct was continuously monitored and controlled to maintain a sample face velocity of  $3 \text{ m min}^{-1}$ . This value was selected to ensure loading times were not unnecessarily long; the results from experiments conducted at the usual operating face velocity ( $1.5 \text{ m min}^{-1}$ ) showed no significant differences for nominally identical samples.

Precise control of both of the air flow rates and the speed at which the salt stick was fed to the thermal generator was maintained throughout. In order to establish the reproducibility of the aerosol concentration, commissioning trials were conducted using samples of a "standard" glass fibre based paper commonly used in HEPA filter production within the UK. Variations of  $< 10 \%$  were observed in the amount of salt collected over a 32 minute test. This permitted the relative performance of the candidate media to be assessed by simply comparing the changes in differential pressure with time.

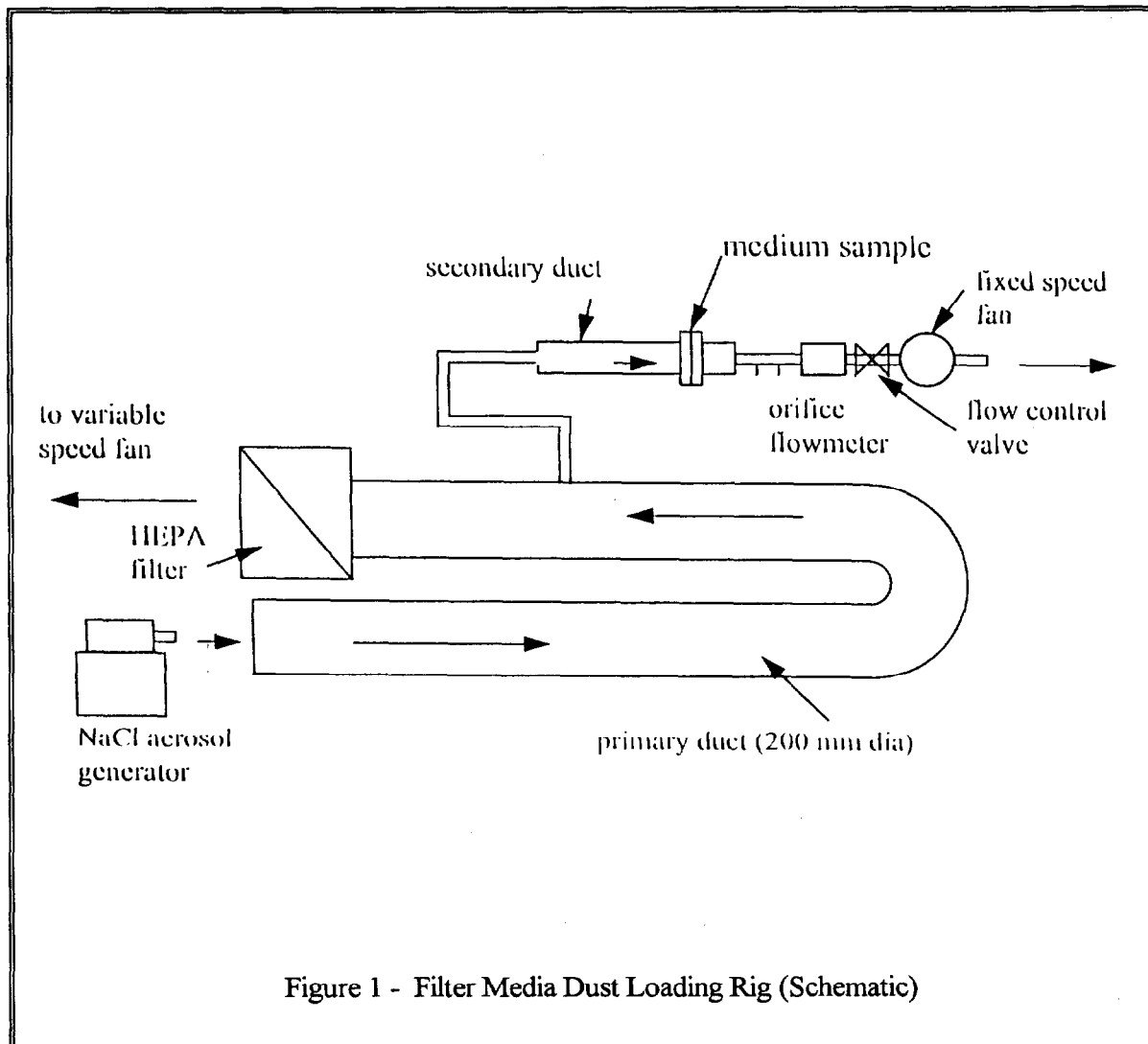


Figure 1 - Filter Media Dust Loading Rig (Schematic)

## 2.2 Filter Testing

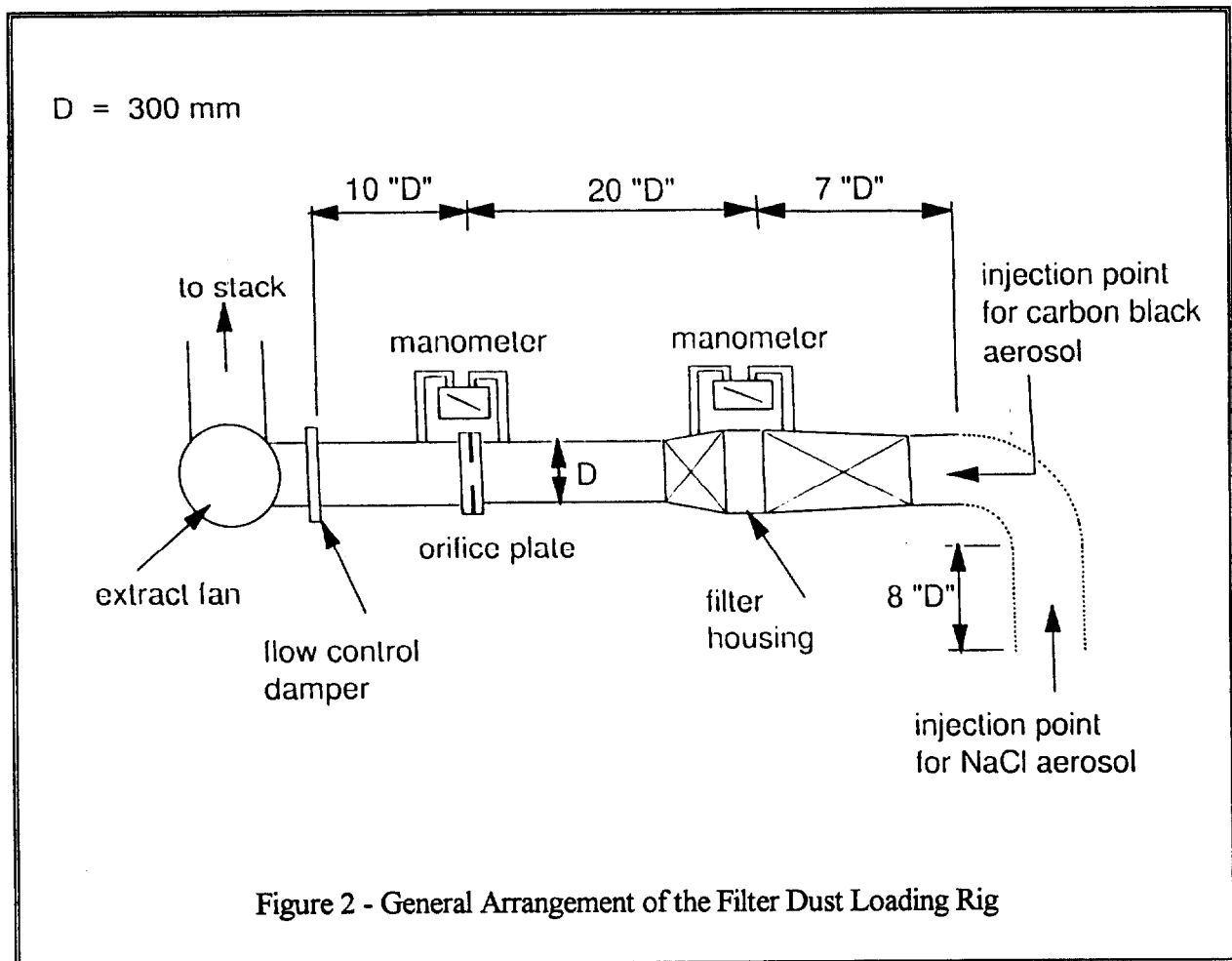
The results from phase 1 of the programme were used to identify the most appropriate media to have incorporated into conventional deep-pleat filters, generally conforming to the requirements detailed in reference 1. The dust loading characteristics of these prototype filters were then established and compared with results obtained for deep-pleat filters containing a typical glass fibre paper.

The rig used (Figure 2) was originally constructed to meet the requirements of BS 3928<sup>(4)</sup>. It essentially comprises an open ended circular inlet duct, which receives the discharge from the aerosol dispenser, a standard filter housing and an outlet duct connected to the extract fan. Air flow rate was maintained at  $1,700 \text{ m}^3\text{h}^{-1}$  during dust loading, and the differential pressure generated across the filter was continuously monitored.

Filter loading trials were conducted using two test aerosols:

## 23rd DOE/NRC NUCLEAR AIR CLEANING AND TREATMENT CONFERENCE

- (a) thermally generated sodium chloride particles (as used for the media loading tests), fed at a rate of 0.33 g/min;
- (b) carbon black (Acetylene 50% compressed) particles, fed at 2.4 g/min. Although the carbon black used was intrinsically sub-micron in size, significant agglomeration was evident during dispersion. The mmd of the resulting aerosol was measured, using an Andersen Cascade Impactor, to be 2.2  $\mu\text{m}$ .



Dust loading was continued until the test filter pressure differential reached 1 kPa and 3 kPa for experiments involving the salt and carbon black aerosols respectively.

### 3. Results and Discussion

The dust loading characteristics of samples cut from a roll of a "standard" HEPA quality paper were routinely measured. This approach enabled the correct operation of the rig to be confirmed by reference to the results obtained for this material. Moreover, the relative dust holding capacity (RDC) of the test medium could be expressed as the ratio of its final pressure drop to the final pressure drop recorded for the standard paper, ie:

$$RDC = \frac{\Delta P \text{ Standard Paper}}{\Delta P \text{ Test Medium}}$$

Although this ratio did not fully quantify differences in the dust holding capacities of the papers, it allowed rapid identification of media for further investigation. Values > 1 indicated an improvement in dust holding. Approximately 40 different media were tested and ratios ranging from 0.6 to 2.0 were recorded.

Figure 3 shows examples of the loading curves obtained. The samples designated F-01 and F-18 are examples of "graded density" papers supplied by Whatman International Ltd. These papers are not commercially available, and were supplied as "development grades". Their structure differs from the uniform density normally associated with standard glass fibre papers. A continuous layer of very fine fibres is supported on a layer of coarser fibres which provide mechanical strength and act as a protective pre-filter. The results illustrated (Figure 3) are for dust loading from the pre-filter side. As may be expected, loading in the reverse direction was observed to nullify the advantage provided by the graded structure.

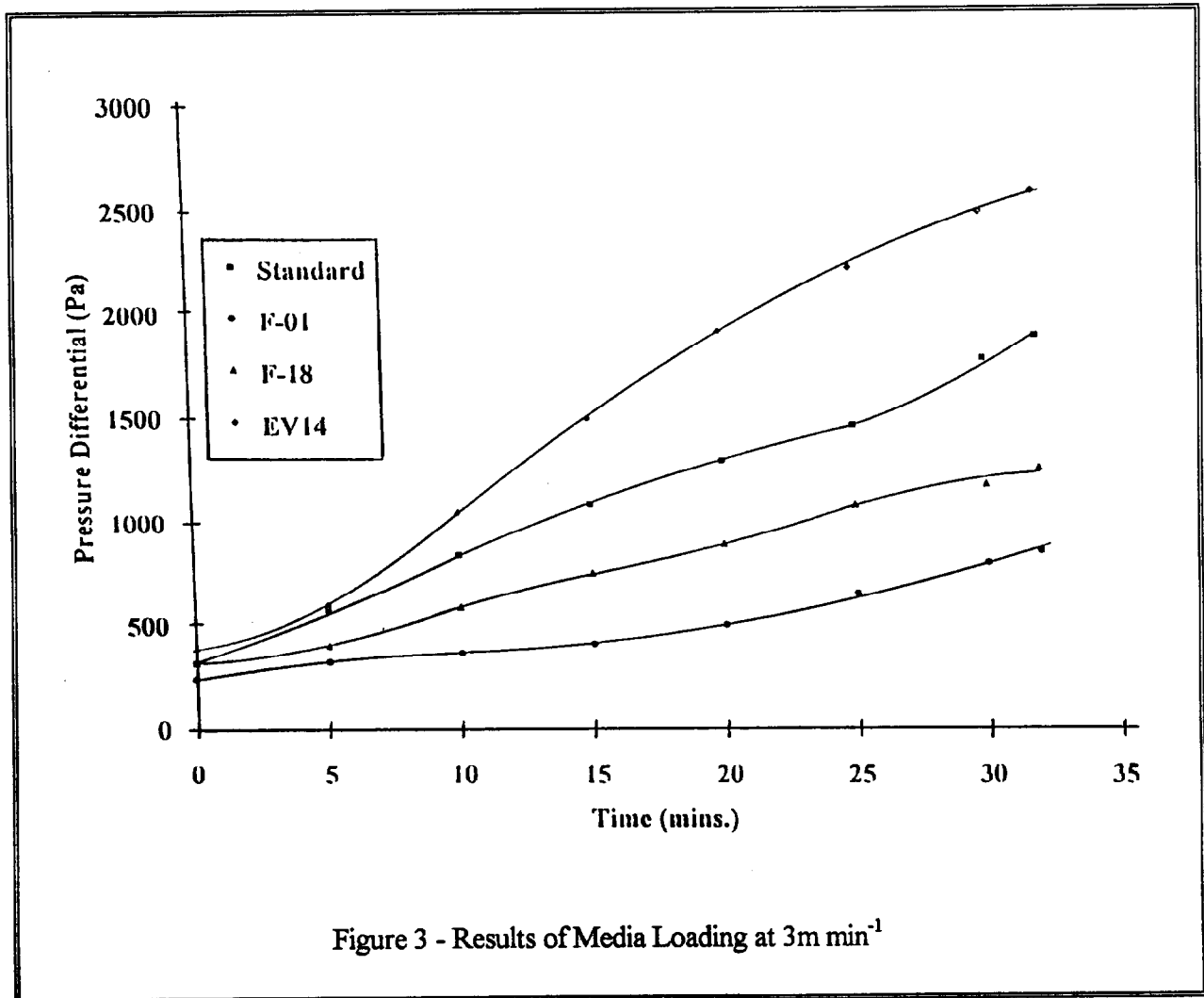


Figure 3 - Results of Media Loading at 3m min<sup>-1</sup>



Although the potential advantage offered by the F-01 paper was established early in the programme, a number of its properties failed to meet the requirements stipulated in AESS 30/93400<sup>(3)</sup> (see Table 1). However, the manufacturing process allows the production of graded media to meet specific requirements in terms of filtration efficiency, strength and dust holding performance. Paper F-18 is the result of a development programme undertaken by the manufacturer to improve the strength properties of the F-01 medium. The increase in strength resulted in some reduction in dust holding, but it is felt that further development will achieve the optimum balance between strength and dust loading characteristics.

Table 1

Physical Property Data for Graded Density Papers

Property	Requirement (AESS 30/ 93400)	Paper Type	
		F-01	F-18
Tensile Strength <sup>(5)</sup> (kNm <sup>-1</sup> ):			
Machine Direction	> 0.8	0.9	1.2
Cross Direction	> 0.5	0.5	0.6
Creased	> 0.5	0.4	0.7
Air Burst Resistance (kPa)	>5.4	> 8.0	> 8.0
Grammage (gm <sup>-2</sup> )	> 85	72	95
Water Repellency (kPa)	> 2.5	0.5	3.1
Thickness (mm)	-	0.51	0.53
Particle penetration <sup>(6)</sup> (%)	< 0.005	0.013	0.003

Influences such as the deposition of dust between the pleats have been shown to adversely affect filter dust holding<sup>(2, 7)</sup>. This suggests that any advantage in the dust loading characteristics of the medium may not be fully realised in the performance of the filter. The experimental filters used in the second phase of the programme were fabricated to include the F-01 and F-18 papers; the dust loading performance of these papers was well characterised, and their use enabled such factors to be quantified.

Dust loading was assessed by comparison with filters manufactured to include the standard glass fibre paper used in the medium selection trials. In all cases the filters were fabricated to incorporate 23± 1 m<sup>2</sup> of paper. The initial BS 3928 penetration values are summarised in Table 2.

In general the penetration results recorded for the filters fabricated from the graded density papers fail the requirement (< 0.01%) stipulated in the relevant specification. However, it is considered that further medium developments can also improve this situation. No significant

## 23rd DOE/NRC NUCLEAR AIR CLEANING AND TREATMENT CONFERENCE

increases in penetration were measured after filter dust loading, and there was no evidence of test dust in the downstream ducting etc.

The sodium chloride and carbon black filter loading results are illustrated in Figures 4 and 5 respectively. In each case the dust load per unit area of media has been calculated and the results are summarised in Table 3. The data presented are based on the nominal area of the media, and do not make allowance for the paper which is in contact with the corrugations of the spacers.

Table 2

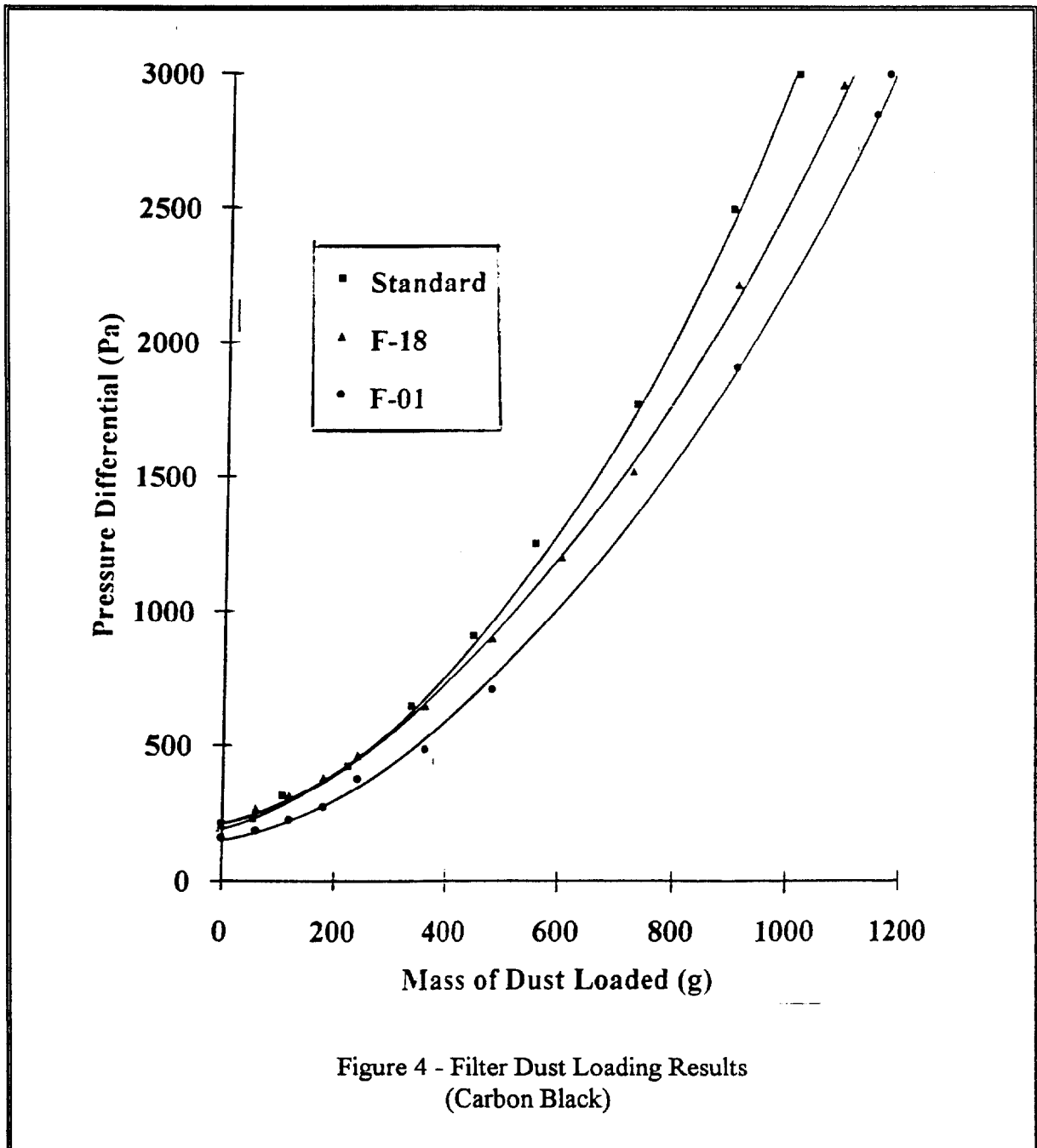
Filter Penetration and Pressure Drop Results

Filter No	Medium Used	$\Delta P$ (Pa)	Pen (%)
7178	Standard	204	0.005
7181	Standard	204	0.003
7461	F-18	201	0.003
7462	F-18	186	0.049
7463	F-01	154	0.026
7464	F-01	154	0.044

Table 3

Filter Dust Load as a Function of Medium Area

Medium	Dust load / Unit area	
	Carbon Black (g m <sup>-2</sup> at 3 kPa)	Sodium Chloride (g m <sup>-2</sup> at 1 kPa)
Standard	43.1	5.3
F-18	47.3	6.6
F-01	48.5	8.2

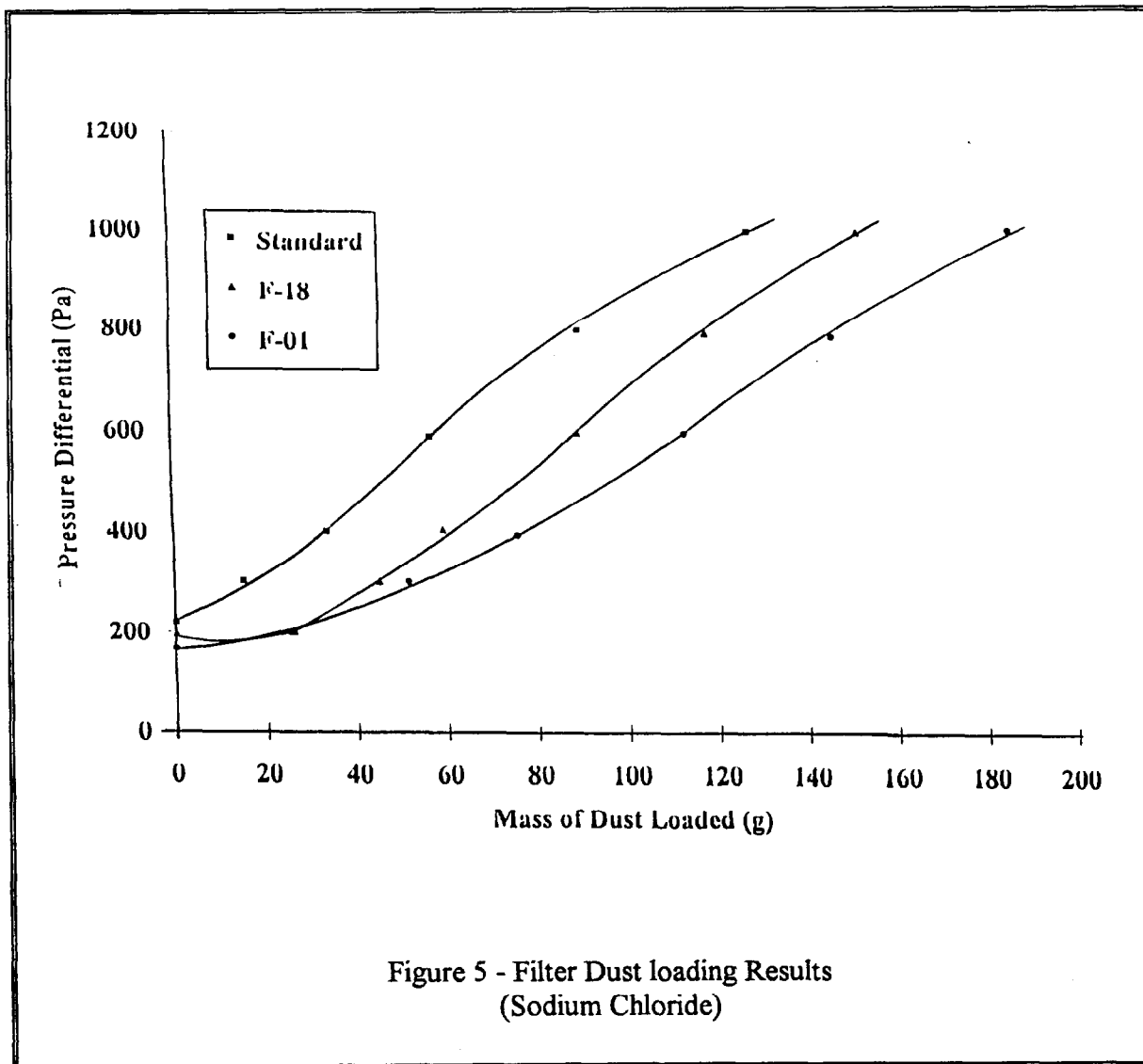


The proportionate differences in filter dust holding capacity (expressed in terms of dust capacity per unit area of medium) are less for carbon black than for the much finer sodium chloride particles. For carbon black the improvements were 25% and 12% at 1KPa for the F-01 and F-18 papers respectively. The improvements in filter loading, for sodium chloride were 55% and 25%. The corresponding values for the sheet media were 95% and 45% respectively.

Clearly, the potential advantages in dust holding offered by the papers have not been realised in the filters. There was noticeable deposition of carbon black within the filter channels; but virtually no deposition observed with the sodium chloride aerosol. Similar differences between

the medium and filter loading data were observed for the standard paper. Further work is necessary to fully quantify these effects.

The distinguishing characteristic of these particular graded density papers appears to be their influence on the changes in paper resistance during the initial particle deposition process. This is illustrated by the shape of the resistance curves in Figure 5. There appears to be a "once only" bonus effect, whereby the graded layer can absorb particles (in this instance up to  $2.0 \text{ gm}^{-2}$ ; approximately  $1 \times 10^{-6} \text{ m}^3$  per  $\text{m}^2$ ) without significant increase in resistance to flow. The resistance then begins to rise and continue in a similar manner to the clean standard paper, ie the resistance rises as though for "cake deposition. In the case of the carbon black results this effect is not apparent.



This suggests that the structure of the graded paper can be expected to influence the increase in resistance due to dust deposition only while the deposit is forming within the depth of the

## 23rd DOE/NRC NUCLEAR AIR CLEANING AND TREATMENT CONFERENCE

medium. Clearly this situation will be most marked in situations where the aerosol is within the most penetrating particle size range.

Such loading characteristics are likely to be most beneficial when HEPA (or ULPA) filters are operated in situations where the allowable increase in operating resistance is restricted, or when very small changes in resistance over a long period of operation are of particular advantage.

### 4. Conclusions

An initial programme to develop a HEPA filter with improved dust loading characteristics has been completed. This work has shown that:

- the relative dust holding of media samples can be rapidly assessed by comparing the increases in pressure differential under standard dust loading conditions;
- graded density glass fibre papers can offer significant improvements in dust holding. Recent manufacturing developments have provided examples of these materials which meet the requirements of the current filter medium specification;
- graded density papers can be incorporated in a standard sized deep-pleat filters. The resulting improvements in filter dust holding are comparable to the advantages demonstrated by the media.
- the increases in dust holding capacity achieved to date have the potential to significantly reduce waste arisings in applications where the challenge is predominantly sub-micron in size.

### 5. References

1. AESS 30/93402 "Filter inserts high efficiency particulate air (HEPA) rectangular deep-pleat 100 - 500 litres/second capacities", March 1990
2. D. Loughborough "The dust holding capacity of HEPA filters". 21<sup>st</sup> DOE/NRC Nuclear Air Cleaning Conference.
3. AESS 30/93400 "Filter medium for use in high efficiency particulate air (HEPA) filters/inserts", August 1989.
4. BS 3928 - "Method for sodium flame test for air filters".
5. BS 4415 - "Determination of the tensile properties of paper and board".
6. BS 4400 - "Sodium chloride particulate test for respirator filters".

7. RP Pratt and BL Stewart "Collection of aerosols in HEPA filters". 19<sup>th</sup> DOE/NRC Nuclear Air Cleaning Conference.

#### 6. Acknowledgements

This work was undertaken with financial support from the UK Department of Trade and Industry, under the management of the Research, Development and Strategy Department of the DRAWMOPS Directorate, at Harwell. The authors gratefully acknowledge the work of Whatman International Ltd in the development of the graded density papers used, and the kind co-operation of MC Air Filtration Ltd in the production of the deep-pleat filters for testing.

\* \* \*

*Effect of humidity on the filter pressure drop*

J. VENDEL, P. LETOURNEAU

Institut de Protection et de Sûreté Nucléaire  
Département de Protection de l'Environnement et des Installations  
Service d'Etudes et de Recherches en Aérocontamination et en Confinement  
IPSN/CEA - 91191 Gif-sur-Yvette Cedex FRANCE

Abstract

The effects of humidity on the filter pressure drop have been reported in some previous studies in which it is difficult to draw definite conclusions.

These studies show contradictory effects of humidity on the pressure drop probably due to differences in the hygroscopicity of the test aerosols.

The objective of this paper is to present experimental results on the evolution of the filter pressure drop versus mass loading, for different test aerosols and relative humidities. Present results are compared to those found in various publications.

An experimental device has been designed to measure filter pressure drop as the function of the areal density for relative humidity varying in the range of 9 % to 85 %. Experiments have been conducted with hygroscopic (CsOH) and nonhygroscopic aerosols (TiO<sub>2</sub>). Cesium hydroxyde (CsOH) of size of 2 μm AMMD has been generated by an ultrasonic generator and the 0.7 μm AMMD titanium oxyde has been dispersed by a "turn-table" generator.

As it is noted in the BISWAS'publication [3], present results show, in the case of nonhygroscopic aerosols, a linear relationship of pressure drop to mass loading. For hygroscopic aerosols two cases must be considered : for relative humidity below the deliquescent point of the aerosol, the relationship of pressure drop to mass loading remains linear ; above the deliquescent point, the results show a sudden increase in the pressure drop and the mass loading capacity of the filter is drastically reduced.

I. Introduction

In Nuclear Industry Particulate Air filters are always used as particulate containment device in gas cleaning and ventilation systems. In some postulated accident scenarios associated with water cooled nuclear reactor, a large quantity of steam could also be released along with a variety of aerosol. The interaction of water vapor with generated aerosols may significantly affect the ability of a filtration system to contain the radio-active aerosols.

Previous studies report [1] [2] contradictory effects of humidity on the pressure drop across filters. They have indicated trends but no definite conclusions could be drawn about the effects of relative humidity on the alteration of pressure drop.

The effects of the relative humidity on the filter pressure drop are bound to be dependant on the hygroscopicity of the particles and may also depend upon the particle size.

The objective of this paper is to present experimental results on the effects of humidity on the pressure drop-mass loading characteristics of a metallic filter according to the particle hygroscopicity. Experiments were conducted using different particle materials : non hygroscopic titanium oxyde and hygroscopic sodium chloride and cesium hydroxyde.

II. Experimental test rig

An experimental test rig, figure 1, was designed to measure the pressure drop across the metallic filter as a function of mass loading (mass/unit area of filter).

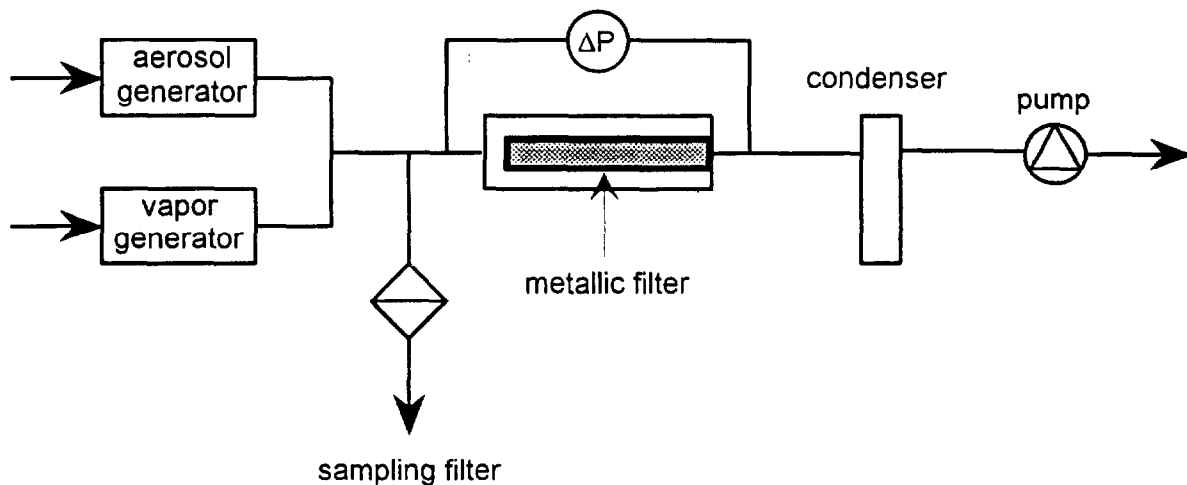


Figure 1 : Experimental test rig



The sodium chloride (NaCl) and cesium hydroxyde (CsOH) aerosols were generated by an ultrasonic atomisation of aqueous solutions of NaCl and CsOH. The droplets formed were drained and dried in an additional dry air flow rate. Titanium oxide powder were dispersed by a "turn table" generator.

In dry air conditions, an Andersen MKII impactor was used to determine the size distribution of the different test aerosols. The measured size distributions were lognormally distributed and the aerodynamic mass median diameters (AMMD) and the geometric standard deviations ( $\sigma_g$ ) are listed in table 1.

Aerosol	AMMD( $\mu\text{m}$ )	$\sigma_g$
NaCl	2.2	1.45
CsOH	2.4	1.50
TiO <sub>2</sub>	0.7	1.55

Table 1 : Particles characteristics

The dry aerosol stream was inlet into the main test rig where the metallic filter was installed in a cylindrical cartridge. The metallic filter had a cylindrical shape of 6 cm in diameter and 30 cm long. The nominal filtration velocity used in these experiments was 5 cm/s.

A known flow rate of humidified air, delivered by a vapor generator, was inlet into the test rig in order to obtain different relative humidities.

Upstream the metallic filter, a sampling tube was installed and connected to a 47 mm filter holder. Glass fiber HEPA filters were used to determine the aerosol mass concentration during the mass loading experiments.

### III. Results and discussion

For the different mass loading tests on the metallic filter the areal loading density (mass/unit area of filter) was computed from the aerosol mass concentration measurements performed on the 47 mm glass fiber filter. The pressure drop across the metallic filter was recorded all along the experiment.

#### Results for the titanium oxyde particles

The pressure drop across the filter was plotted as a function of areal loading density. The results are presented in figure 2 for tests performed under dry air conditions and at RH of 85 %; the pressure drop versus mass loading curves are linear and no significantly variation in the slopes of these curves can be observed. Similar observations have been made by BISWAS [3] for nonhygroscopic particles of 0.5  $\mu\text{m}$  in diameter below a RH of 90 %.

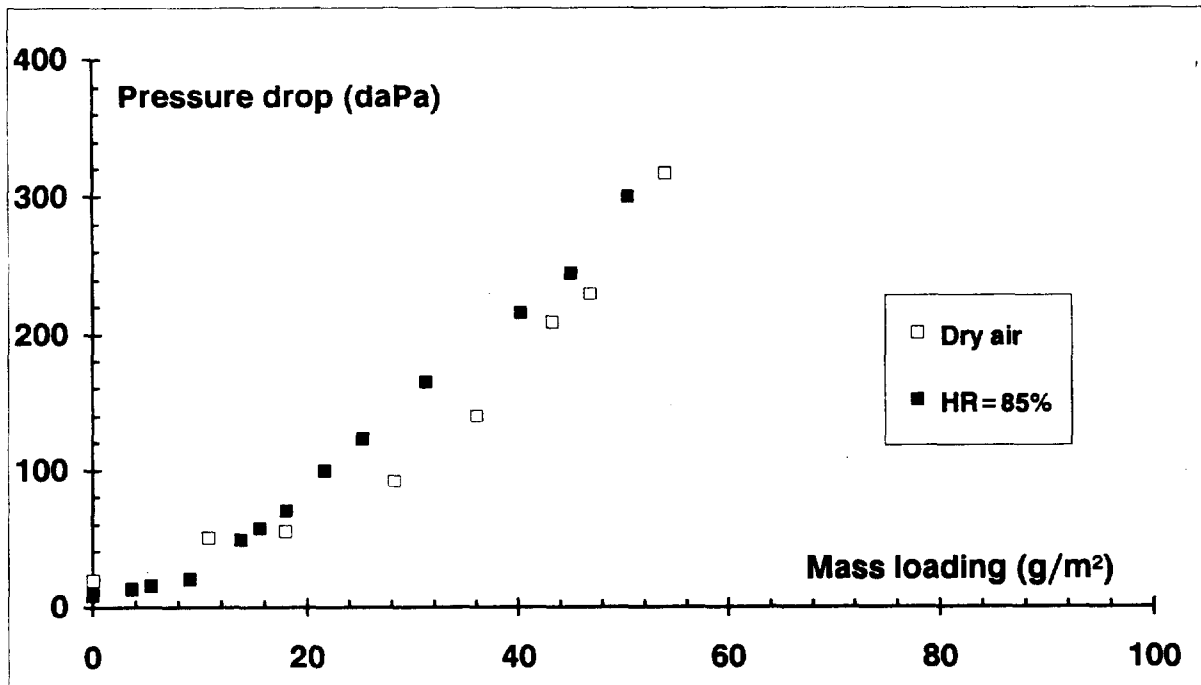


Figure 2 : Measured pressure drop versus areal density for titanium oxyde particles

Results for the NaCl particles

In figure 3 are presented the results of the mass loading experiments performed with a hygroscopic aerosol (NaCl) under dry air conditions and at RH of 23 % and 85 %.

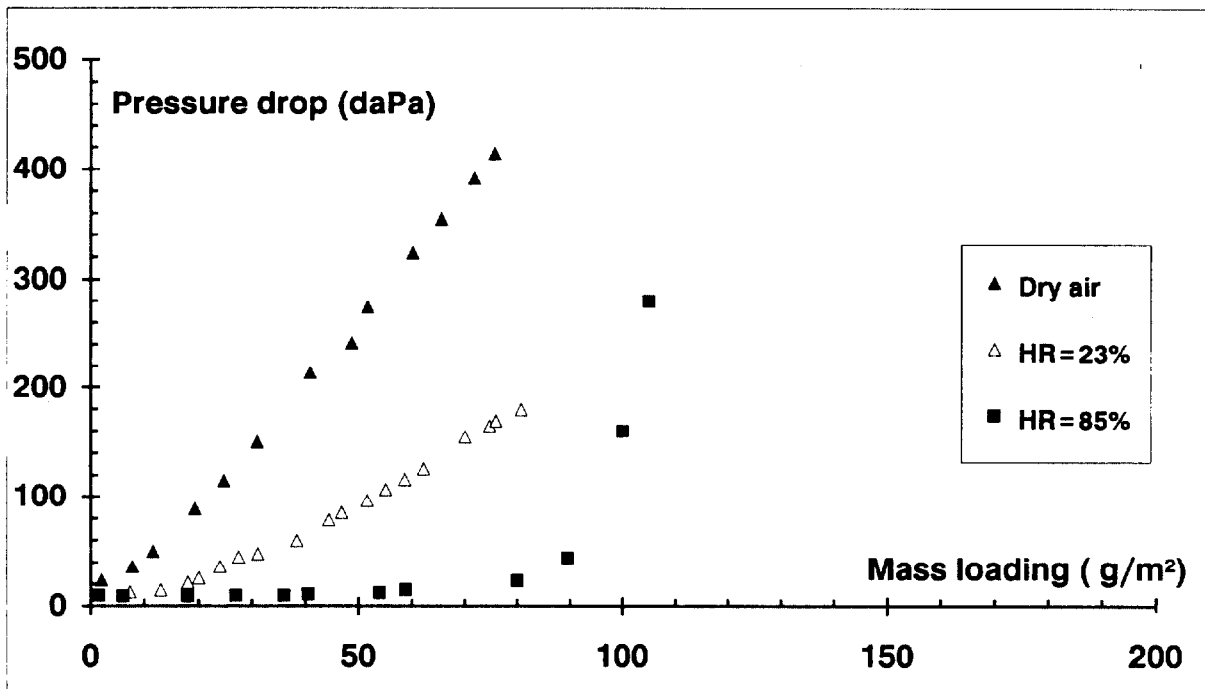


Figure 3 : Measured pressure drop versus areal density for sodium chloride particles

For dry air conditions and at RH of 23 %, a linear relationship of pressure drop to mass loading was obtained. At RH of 85 % this relationship was non-linear and it was observed a sudden increase in pressure drop.

These kind of results were also observed by BISWAS [3] and they show that the non-linear curves were only obtained for NaCl aerosol tests at humidities higher than the deliquescent point (RH = 75 %)

Results for the CsOH particles

For different humidities ranging from 9 % to 85 %, the results of the mass loading experiments performed with CsOH particles are presented in figure 4. On this figure the results obtained under dry air conditions are also noted.

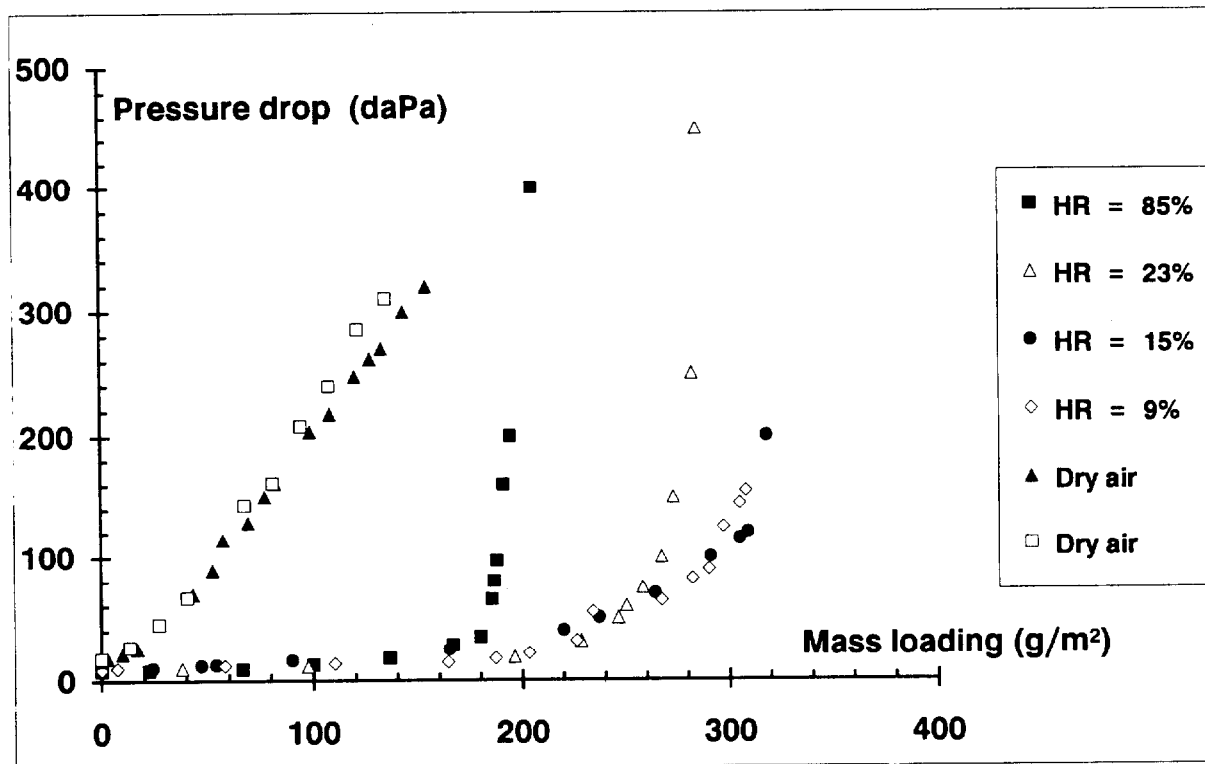


Figure 4 : Measured pressure drop versus aeral density for cesium hydroxyde particles

For dry air condition a linear relationship is observed. Because the deliquescent point for the CsOH-H<sub>2</sub>O system [4] in the temperature range 20°C-100°C is about 2 % RH, non linear relationship of pressure drop to mass loading was obtained.

As the figure 4 shows, the sudden increase in pressure drop seems initiated at lower mass loading when the relative humidity is increased.

IV. Conclusion

The objective of the study was to present experimental results of the effect of humidity on the evolution of the filter pressure drop versus mass loading.

Linear relationships of pressure drop were obtained for non hygroscopic aerosols and for hygroscopic aerosols at humidity below the deliquescent point. Moreover a decrease in pressure drop with mass loading in humidity conditions has been observed for the hygroscopic NaCl particles. For RH of 85 % ,this trend has not been noted for the non hygroscopic titanium oxyde particles.

Above the deliquescent point, non-linear relationship of pressure drop versus mass loading have been observed for hygroscopic NaCl and CsOH particles. In the case of CsOH particles, the sudden increase in pressure drop could make the filter completely clogged. The effect of humidity above the deliquescent point is to reduce the mass loading capacity of a filter. Hence to avoid filter clogging, caution must be exercised in filtration of hygroscopic aerosols at humidities above their deliquescent point.

REFERENCES

- [1]T. ARIMAN, D.J. FIELFRITCH  
Filtration and separation 14, 127-130 (1977)
- [2]P. SMITH, T.S. SCHLUTHEIS, J. WALLS, W. GREGORY  
21<sup>st</sup> DOE/NRC Nuclear Air Cleaning Conference  
San Diego PP 366-375 (1990)
- [3]A. GUPTA, V.J. NOVICK, P. BISWAS, P.R. MONSON  
Effect of humidity and particle hygroscopicity on the mass loading capacity of HEPA filters  
Aerosol Science and Technology 19-94-107 (1993)
- [4]J. JOKINLEMI, K. KOLSTINEN, T. RAUEMAA  
Experimental verification of hygroscopic aerosol growth in reactor accident conditions  
Nuclear Technology, june 1990

DISCUSSION

**WEBER:** Did you have a chance to see what would happen after drying out a filter that had clogged because it was operated above the deliquescent point of the contaminant? Did the pressure drop change?

**VENDEL:** We did not make this kind of experiment. I don't know if the pressure drop changes when you dry the filters.

**TSAL:** In the last slide and the previous one, there is something that is difficult for me to understand. The 85% RH curve is a horizontal line close to zero pressure drop until it rises abruptly. To me this means that if I increase humidity I will bring the resistance down below what it would be in dry air until the sudden rise. Is it right? At 85% RH, your pressure drop is not increasing when you load the filter more and more.

**VENDEL:** Above the deliquescent point, the pressure drop does not increase with mass loading. One of the explanations is that a liquid film is formed on the fibers of the filter. In the case of cesium oxide, it is not necessary to have a relative humidity of 85%. This trait is also observed for humidity of about 9%. When you work above the deliquescent point, the pressure drop of the filters does not increase according to the mass loading, and a sudden increase in pressure drop can appear. In the case of cesium oxide, the filter is completely clogged and we can't work with these filters. It is not necessary to have 85%; it is strained when you work above the deliquescent point of the material that you use.

**TSAL:** It is very hard to understand because we are not used to this. We now understand that when you have a higher RH, resistance will be less until you plug the filter and then it becomes too wet. This is very important data because we do not take enough care about RH when calculating HVAC systems.

**BERGMAN:** Does the mass loading include the water content, or is it only particles? You plot pressure drop versus mass loading. Is that the weight of the filter when it's wet, or did you put it in an oven and then weigh it?

**VENDEL:** Yes, the mass loading presented includes water so the filters are weighed directly without any drying sequence.

Preliminary Field Evaluation of High Efficiency Steel Filters\*

by

W. Bergman, G. Larsen, R. Lopez and K. Wilson  
Lawrence Livermore National Laboratory  
P.O. Box 5505, Livermore, CA 94550  
and

K. Simon and L. Frye  
Martin Marietta Energy Systems Inc  
Oak Ridge Y-12 Plant, Oak Ridge, TN 37831

ABSTRACT

We have conducted an evaluation of two high efficiency steel filters in the exhaust of an uranium oxide grit blaster at the Y-12 Plant in Oak Ridge Tennessee. The filters were installed in a specially designed filter housing with a reverse air-pulse cleaning system for automatically cleaning the filters in-place. Previous tests conducted on the same filters and housing at LLNL under controlled conditions using Arizona road dust showed good cleanability with reverse air pulses.

Two high efficiency steel filters, containing 64 pleated cartridge elements housed in the standard 2' x 2' x 1' HEPA frame, were evaluated in the filter test housing using a 1,000 cfm slip stream containing a high concentration of depleted uranium oxide dust. One filter had the pleated cartridges manufactured to our specifications by the Pall Corporation and the other by Memtec Corporation. Test results showed both filters had a rapid increase in pressure drop with time, and reverse air pulses could not decrease the pressure drop. We suspected moisture accumulation in the filters was the problem since there were heavy rains during the evaluations, and the pressure drop of the Memtec filter decreased dramatically after passing clean, dry air through the filter and after the filter sat idle for one week. Subsequent laboratory tests on a single filter cartridge confirmed that water accumulation in the filter was responsible for the increase in filter pressure drop and the inability to lower the pressure drop by reverse air pulses. No effort was made to identify the source of the water accumulation and correct the problem because the available funds were exhausted.

I. Introduction

This report describes the continuation of our development of a high efficiency particulate air (HEPA) filter that is made from stainless steel medium and is cleanable by reverse air pulses for nuclear air cleaning applications. Our initial study established the feasibility of developing a HEPA filter made from steel fiber medium (1). At that time, commercially available steel media had either a low efficiency or a

---

\*This work was performed under the auspices of the U.S. Department of Energy by Lawrence Livermore National Laboratory under contract no. W-7405-eng.48. The work was supported by DOE's Office of Technology Development, EM-50.

high pressure drop. We evaluated a variety of steel filter media and concluded that media made from steel fibers yield higher efficiencies and lower pressure drops than comparable media made from powder metal. Another major conclusion of that study was that reducing the fiber diameter would simultaneously yield higher efficiencies and lower pressure drops. We then worked separately with Pall Corporation and Memtec of America Corporation to develop a steel fiber medium that had the lowest pressure drop while maintaining a minimum efficiency of 99.97% for 0.3  $\mu\text{m}$  DOP particles. Both Pall and Memtec were able to make a filter medium that met the HEPA efficiency requirement but had a pressure drop of about three inches of water. Although we knew that smaller diameter fibers were needed to achieve HEPA performance for filters having the standard dimension of 2 ft. x 2 ft. x 1 ft., none were available.

Our next step was the development and evaluation of a prototype steel filter using the new media made from 2  $\mu\text{m}$  diameter steel fibers (2). We established the basic design parameters of the filter in a semi-empirical study. To obtain a sufficient filter area, we selected the pleated cartridge design shown in Figure 1. The cartridge parameters of pleat width and pleat depth were selected based on a compromise between maximum filter area and filter cleanability. We then issued contracts to Pall and Memtec to make a sufficient number of cartridges to fabricate a standard 1,000 cfm capacity filter from each company. Figure 2 shows the assembled filter that consisted of 64 cartridge elements. We fabricated two filter units, one using cartridges made by Pall, and the second using cartridges made by Memtec. Both of the filters were certified to have 99.99% efficiency for 0.3  $\mu\text{m}$  DOP particles when tested at 1,000 cfm in the DOE filter test facility at Oak Ridge, Tennessee. The measured pressure drop for the Pall filter was 3.2 inches, while the Memtec filter had a pressure drop of 2.9 inches.

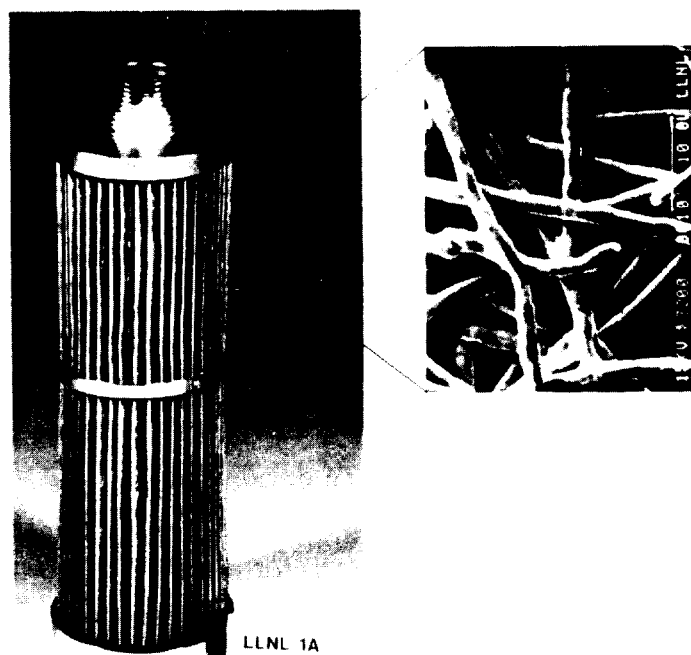


Figure 1. Single filter cartridge and electron micrograph of stainless steel fiber medium.



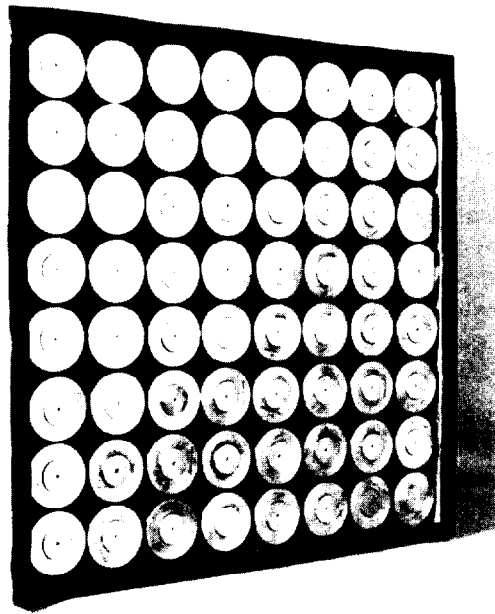


Figure 2. Photograph of the cleanable steel filter consisting of 64 cartridge elements

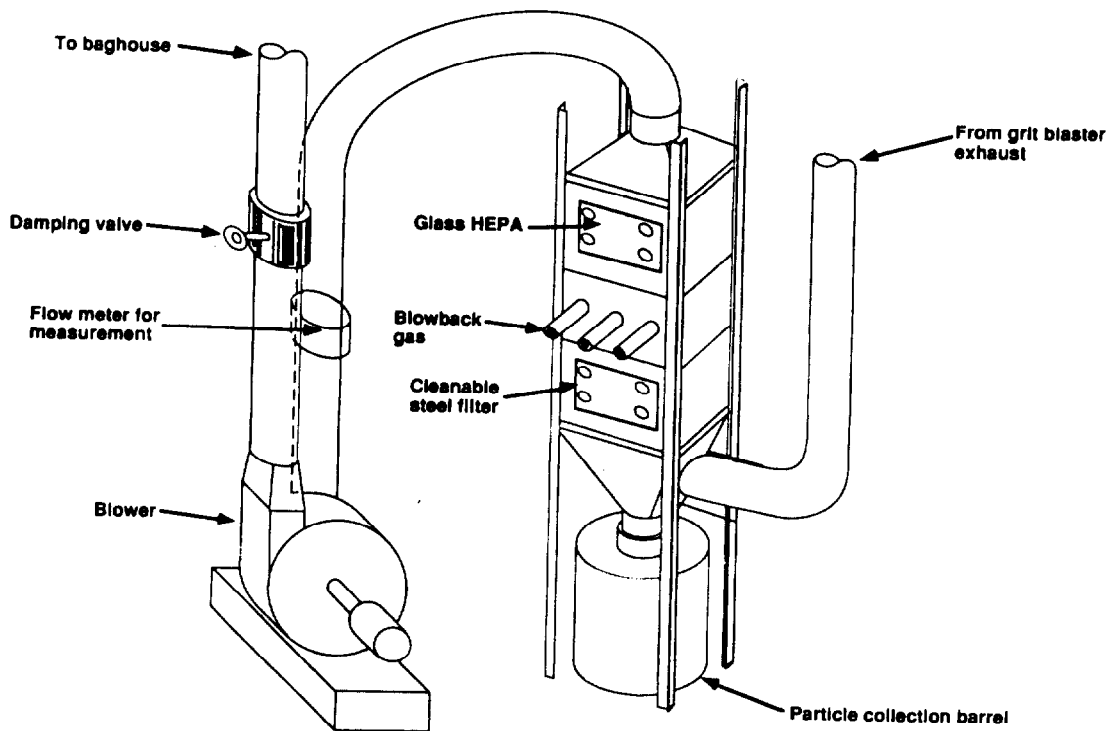


Figure 3. Schematic of the filter housing and blower assembly

The steel filters were evaluated in the filter housing assembly shown in the schematic in Figure 3. The steel filter was housed in the lower chamber. The middle chamber contained the tubing used for air pulse cleaning, and the upper chamber contained a standard glass HEPA filter. Figure 4 shows a photograph of the filter housing and blower assembly. The steel filters were subjected to multiple cycles of dust loading with Arizona road dust and cleaning with reverse air pulses as shown in Figure 5. The filter cleaning is done without interrupting the air flow because only four of the filter cartridges are cleaned at one time. As the dirty air is filtered, particle deposits form on the surface of the filter and cause the pressure drop to increase. After the filter reaches a preset pressure drop, a reverse air pulse blows back through a sequence of four cartridge elements at a time to dislodge the particle deposits, which are then collected in a waste drum. Cleaning tests conducted with Arizona road dust showed that, after the first few cleaning cycles, the filter maintained a constant pressure drop of 5 inches after each pulse cleaning.

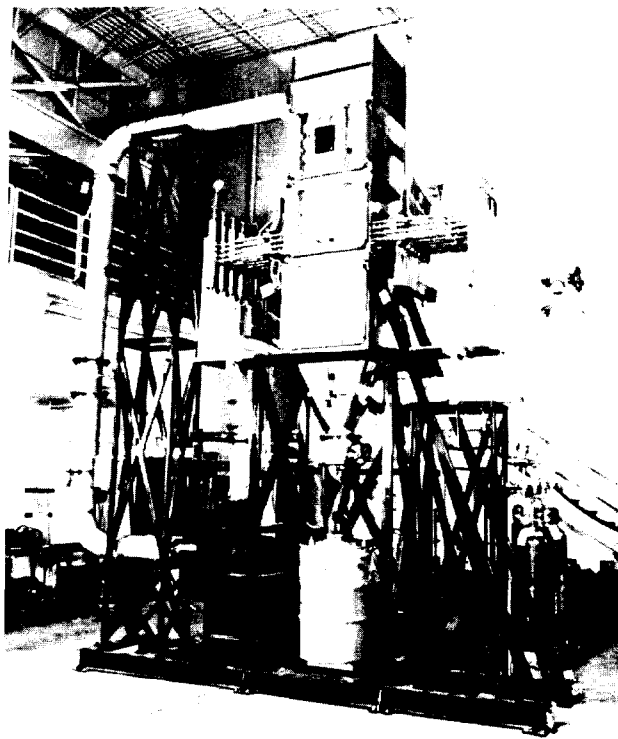


Figure 4. Photograph of the filter housing and blower assembly

## II. Preparation for the Demonstration at the Y-12 Plant

After surveying potential sites at LLNL, Idaho National Engineering Laboratory, and the Y-12 Plant, we selected a grit blaster at the Y-12 Plant as the preferred demonstration site. The grit blaster uses abrasive grit to mechanically remove oxides and surface contamination from depleted uranium billets and other formed parts. The exhaust from the grit blaster first passes through a grit recovery system and then through a bag filter and HEPA filter system shown in Figure 6.

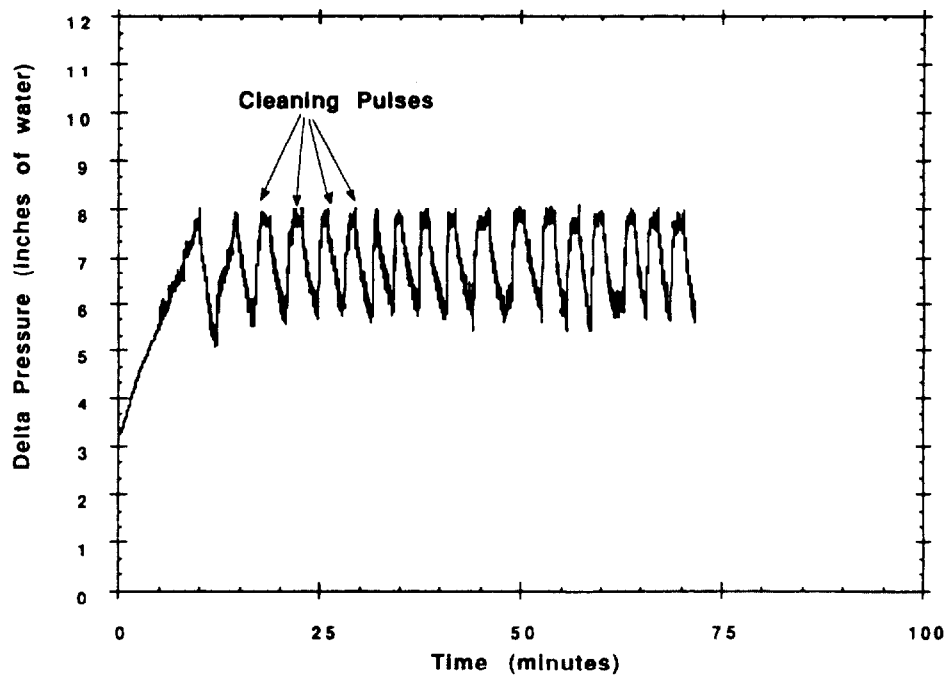


Figure 5. Multiple cycles of filter loading with Arizona road dust and filter cleaning with reverse air pulses.

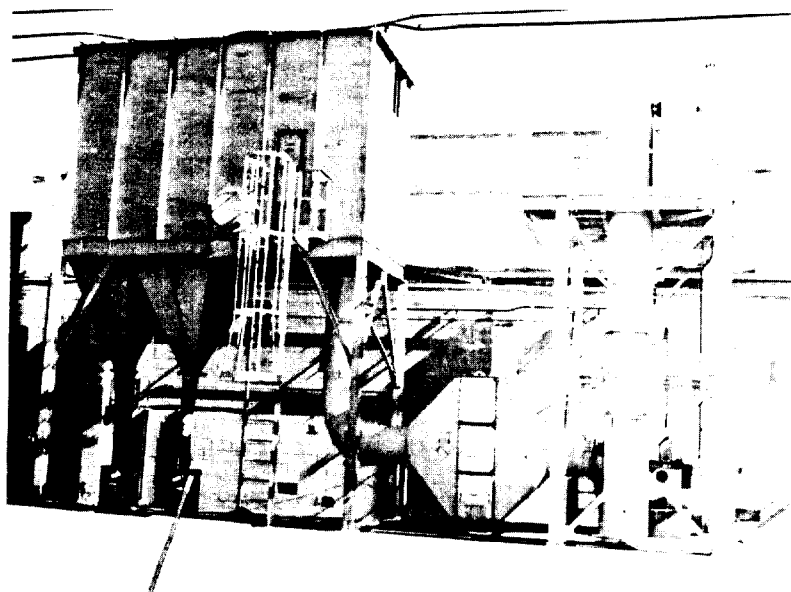


Figure 6. The exhaust system from the grit blaster consists of a bag and a HEPA filtration system.

The exhaust from the grit blaster had many attractive features for our field demonstration. The facility could generate a large quantity of dust on-demand and thereby would allow us to conduct many cycles of filter loading and cleaning in a short time. The depleted uranium oxide served to demonstrate the filter in a radioactive application; but since the radioactivity was very low, the added health and safety requirements from handling radioactive material was minimal. Another attractive feature of the demonstration site was that the grit blaster generates large particles in a dry process. Figure 7 shows a comparison of the uranium oxide dust measured at the Y-12 Plant and the Arizona road dust used in the LLNL filter loading and cleaning tests. The data were obtained with inertial impactors and are plotted as percent mass less than stated size as a function of particle size. The mass median diameter (50% points on the graphs) for the Arizona road dust and the uranium oxide dust is 7.5  $\mu\text{m}$  and 200  $\mu\text{m}$  respectively. The larger size of the uranium oxide dust should make it much easier to clean the steel filter than the smaller Arizona road dust.

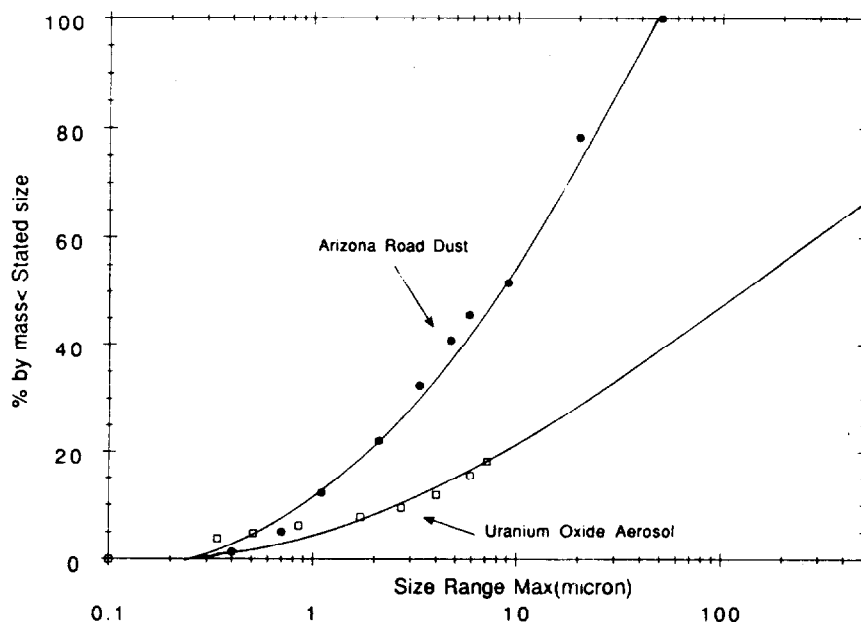


Figure 7. Size distribution measurements show the uranium oxide particles are much larger than the Arizona road dust.

The filter housing assembly was then installed outside the building next to the existing bag filter as seen in Figure 8. A separate 1,000 cfm slip stream was cut into the existing 3,000 cfm exhaust duct from the grit blaster and connected to the inlet of the filter housing assembly (the right vertical duct in Figures 3 and 4). The exhaust from the filter housing assembly was then reconnected to the existing duct leading to the bag house.

Most of the effort in the field demonstration was spent on health and safety reviews and preparations for the tests. In addition to the standard health and safety

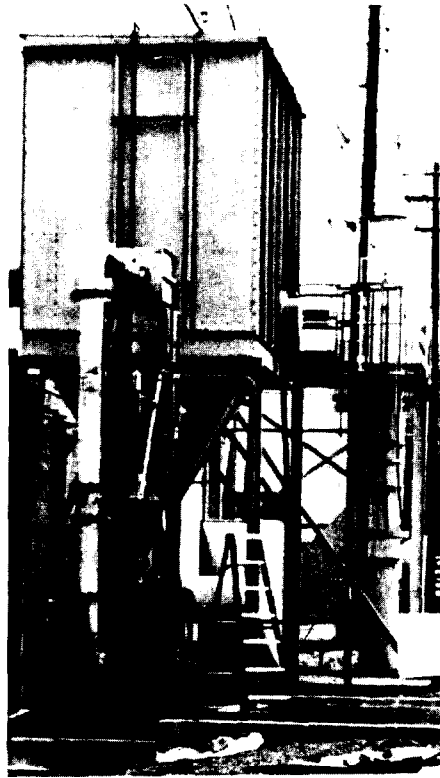


Figure 8 Filter housing assembly for evaluating the cleanable steel filter mounted next to the bag filtration system.

reviews, we conducted a seismic study on the filter housing assembly shown in Figure 4 to insure that the unit would not tip over. Because of the height, scaffolding had to be erected to allow for changing both the steel and the glass fiber filters. We also built an alignment table to support the 200 pound steel filter during filter installation. The alignment table was mounted on a scissors lift.

We also performed leak tests on the filter housing and blower assembly using the constant pressure method in ASME-N510-1989 (3). According to this method the inlet duct was sealed and a dry gas meter was installed between the blower and the exit duct from the glass HEPA. The initial test showed a leak of 0.68 cfm at 10 inches of vacuum, which met the most stringent requirement 0.1% maximum leak specified in Table B-3 in ASME-509 (4). The small leak was determined to come from the manifold plate gasket that supported the air pulse cleaning system. After sealing the leak with Glyptal 1202, the leak was reduced to 0.017 cfm. Leak tests based on ASME N510 were also performed on the two glass HEPA and two, steel, high efficiency filters after installation to insure that the filter leaks did not exceed 0.03%.

### III. Y-12 Test Results Show Filter Plugging, Apparently Due To Moisture

The objective of our tests at the Y-12 Plant was to establish that the steel filter could be repeatedly cleaned in a field demonstration and thereby save the equivalent of 15 or more standard HEPA filters. A standard glass HEPA filter downstream of the

steel filter would verify that the steel filter trapped nearly all of the particles. The pressure drop across this filter remained constant at one inch of water during this evaluation, thereby insuring that virtually all of the particles were trapped on the first filter. The number of steel filter loadings and cleanings that correspond to the life of a single glass HEPA filter would be established in a baseline test of a glass HEPA filter. Details of the field demonstration were reported by Simon and Frye (5).

Figure 9 shows the pressure drop increase with increasing filtration time for one of two baseline glass HEPA filters tested. The HEPA filter was installed in the lower housing compartment on April 28, 1993 and tested for uranium oxide loading on the next day to provide a baseline test for the Memtec filter. Note that the initial pressure drop was 1.5 inches, which indicates a significant plugging even before exposure to the uranium oxide dust. We suspect high moisture was responsible for the high pressure drop based on observations from the subsequent test with the Memtec filter. Removing the filter from the housing at 4 inches of pressure and weighing it showed the filter had increased its weight by 1.7 pounds. We selected 4 inches pressure drop as the typical upper limit pressure drop for replacing HEPA filters. The baseline test for the Pall filter using a different HEPA filter showed a weight increase of 2.4 pounds. That HEPA filter had an initial pressure drop of 0.78 inches. Thus, an average weight gain of 2 pounds of uranium oxide would serve as the reference weight corresponding to one HEPA life.

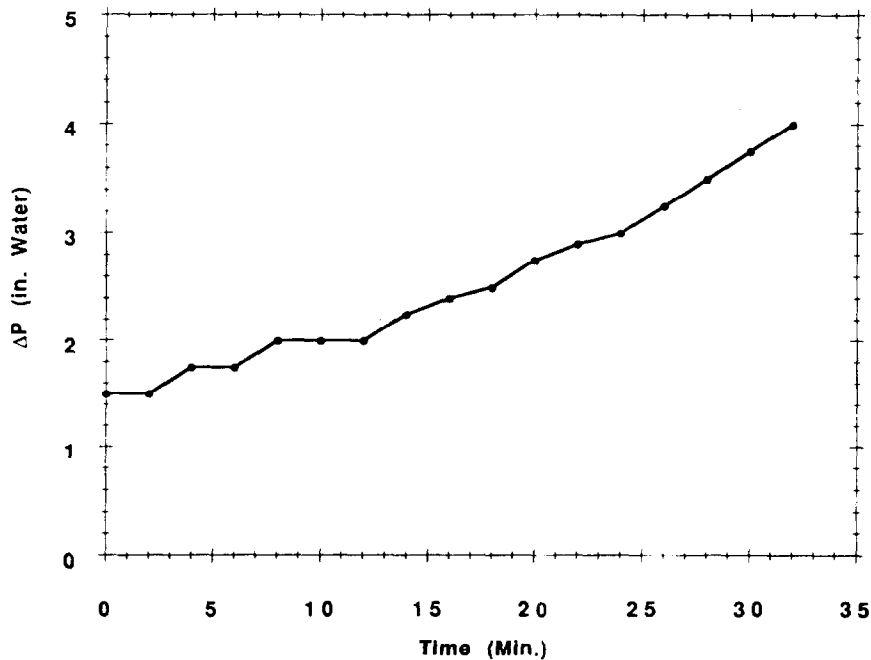


Figure 9. Pressure drop increase in a standard glass HEPA filter during loading with depleted uranium oxide dust.

The steel filter from Pall was installed and tested on April 15, 1993 for particle loading and cleaning. Figure 10 shows the pressure drop increase during the loading and the times where pulse cleaning was applied. Note that the pressure drop did not decrease after the pulse cleanings, indicating that the filter could not be cleaned. Visual examination of the filter showed that virtually no deposits had formed on the

filter surface. This is contrast to the heavy, irregular deposits observed in the LLNL tests with Arizona road dust (2).

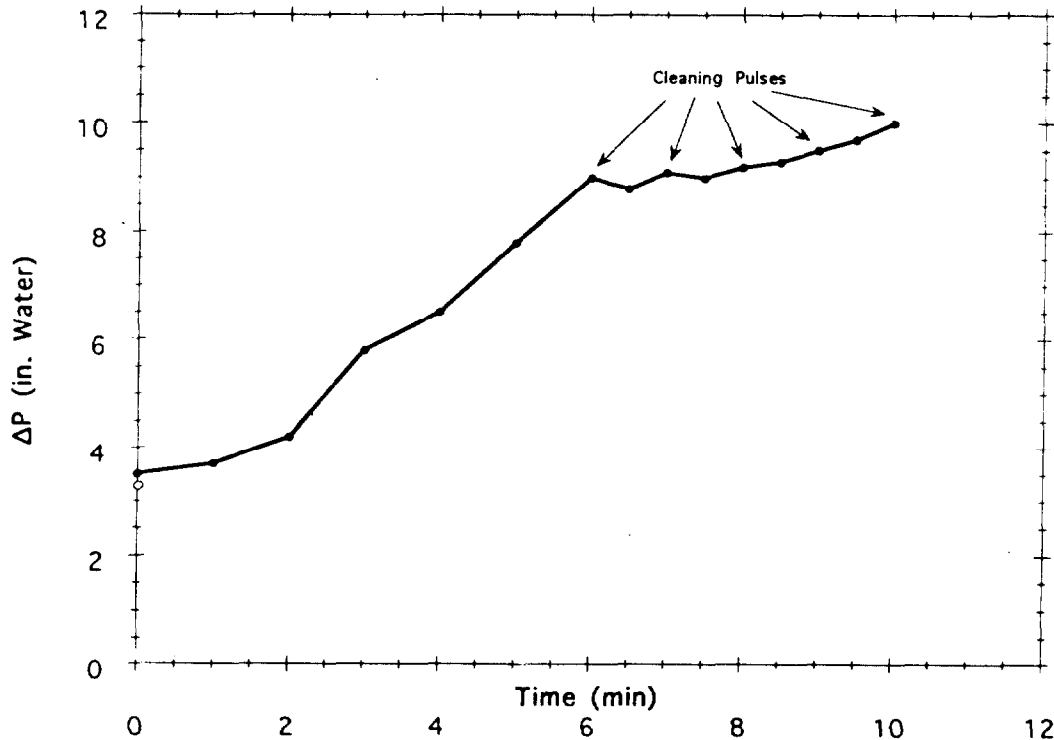


Figure 10. Pressure drop measurements on the Pall steel filter during loading with depleted uranium oxide dust and cleaning with reverse air pulses.

We suspected that moisture may have been responsible for our inability to clean the filter since there was a heavy rainstorm prior to and during the test. There was so much moisture in the system that water condensation had accumulated in one of the Magnahelic pressure gages and displaced the needle from its shaft. The Magnahelic pressure gage was connected to the Pitot tube flow meter that provided flow measurements for the test system. The defective gage was replaced prior to the test on the Pall filter. Unfortunately there were no humidity sensors in the exhaust duct to verify the high moisture content. To correct this deficiency, a humidity sensor was installed in the middle chamber of the filter housing assembly before proceeding with the next test.

The Memtec steel filter was then installed in the filter housing on May 4, 1993 for a new loading and cleaning test. Figure 11 shows the pressure drop across the filter during the field evaluation. Note that the initial pressure drop of the filter at the beginning of the test was 7 inches, which is much higher than the value obtained at LLNL or at the DOE Filter Certification Laboratory in K-25. Since the relative humidity measured after the filter indicated 90%, we suspected the filter was saturated with water, presumably from condensation. We then purged the filter by turning on the air blower without operating the grit blaster for 14 hours. This reduced the pressure drop to a constant 4.5 inches and dropped the relative humidity to 53%.

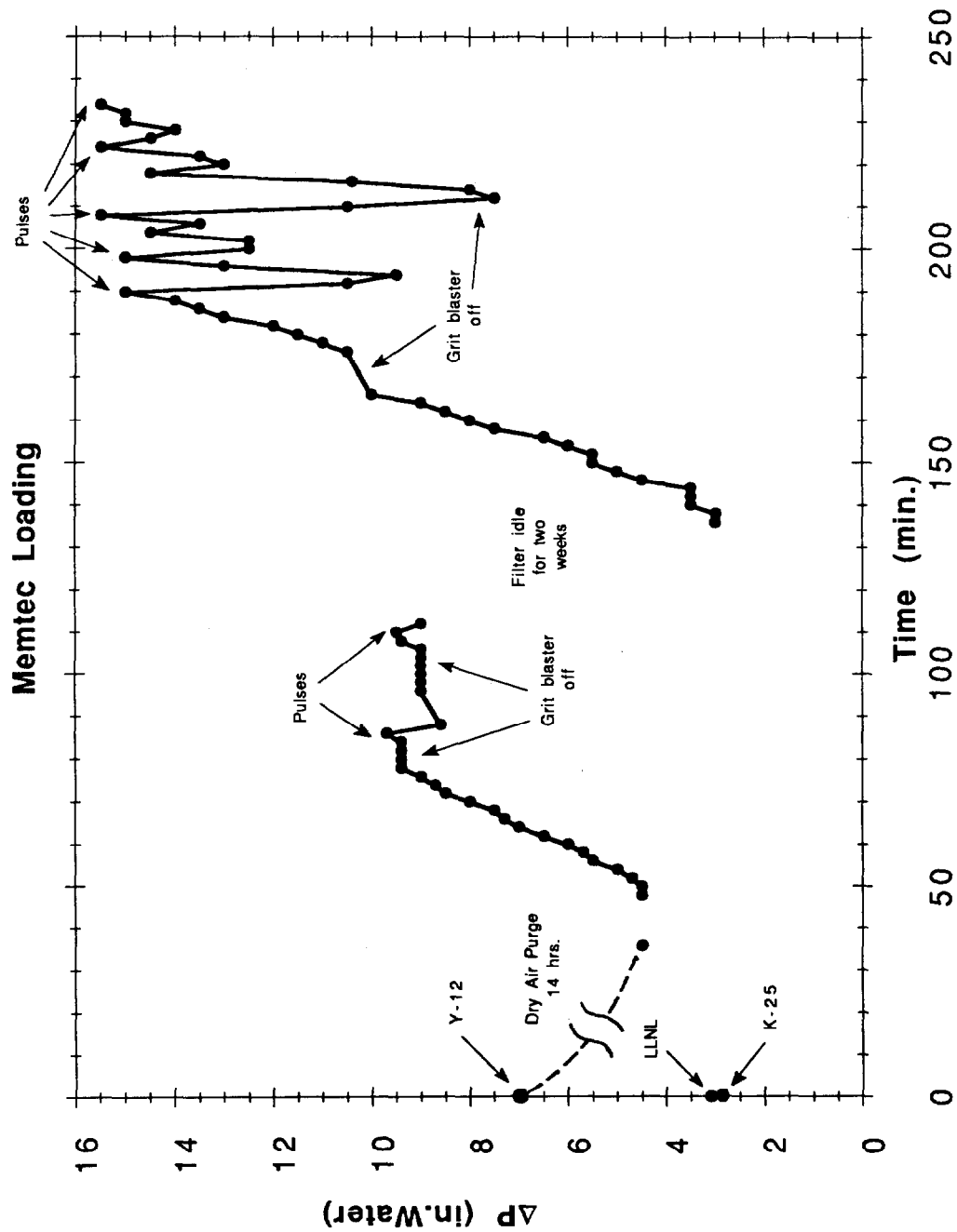


Figure 11 Pressure drop measurements on the Memtec steel filter during loading with depleted uranium oxide dust and cleaning with reverse air pulses.



## 23rd DOE/NRC NUCLEAR AIR CLEANING AND TREATMENT CONFERENCE

The filter loading test was then started by operating the grit blaster on May 7, 1993 with the filter at 4.5 inches. Figure 11 shows the pressure drop increased with time in a similar fashion as the Pall filter in Figure 10. Attempts to clean the filter by reverse air pulses were also not successful; there was only a slight decrease in pressure drop after each pulse. The relative humidity after the filter varied between 48-55%.

We then stopped the loading test for nearly two weeks while we attempted to understand why reverse air pulses would not reduce the pressure drop. One hypothesis was that there was an insufficient dust cake to blow off by reverse air pulses. Visual inspection of the Pall filter in the previous test had confirmed that there was an insignificant deposit on the filter surface. We reasoned that a sufficient layer of particle deposits had not formed and therefore could not be blown off. Allowing the pressure drop to increase to 15 inches instead of 9 inches should increase the amount of particle deposits.

The loading test on the Memtec filter was then continued on May 20, 1993 to see if an increased particle deposit on the filter would make it easier to clean. Figure 11 shows that the filter pressure drop had decreased from 9 inches when the test was stopped to 3 inches when the test was continued. The filter pressure drop increased monotonically with increasing exposure to the uranium oxide stream until the reverse air pulse was activated at 15 inches of water, which reduced the pressure drop to 9.5 inches. The second cleaning had only a small effect. However after the third cleaning, the filter pressure drop decreased from 15 inches to 7.5 inches. The grit blaster was shut off at the same time and may have contributed to the decreased pressure drop. After the grit blaster was reactivated, the filter pressure drop rapidly increased to 14 inches and was not strongly affected by subsequent air pulses. The relative humidity in the filter duct was 44% at the start of the test and varied between 38% and 45% during the test. To verify that the pressure readings were correct, we performed a post-test calibration which showed the pressure gage was reading 0.5 inches lower. The data in this report were corrected for this error.

The following observations of the Memtec filter strongly suggested that water saturation on the filter was responsible for the pressure measurements: The pressure drop increased from 3 inches to 7 inches after installing the Memtec filter in the filter housing. It then dropped to 4.5 inches after passing clean air through the filter for 14 hours. The relative humidity measured after the filter dropped from 90% to 53% during the air purging. This data suggests that water is driven off the filter. The pressure drop also decreased from 9 inches to 3 inches after sitting idle for almost two weeks. Evaporation of water from the filter is the most likely explanation. The final observation that suggests that filter clogging is due to water and not particles is the inability of the reverse air pulses to reduce the pressure drop after filter clogging to either 9 inches or 15 inches.

Since high efficiency filters are not designed to operate under high moisture conditions, the source of the moisture should be identified and reduced. This task was the next logical step in our evaluation. Unfortunately, the field evaluation had to be terminated after the Memtec filter tests because the allocated funds were exhausted.

### IV. Laboratory Tests Confirm Filter Plugging Is Due To Water

Since we could not complete the field evaluation, we conducted a series of laboratory tests on single cartridge filters to verify that water accumulation was responsible for filter plugging and the ineffective cleaning. Figure 12 shows the experimental apparatus used for the filter clogging and cleaning tests. The filter test housing consists of three chambers: a lower chamber that functions as a hopper to collect particle deposits, a middle chamber that houses the filter cartridge and an upper chamber that has the reverse air pulse system. Challenge air enters from the right into the lower part of the middle chamber, passes through the filter cartridge into the upper chamber and then leaves through the exit port on the left. Relative humidity measurements were made by replacing the sample probe in the middle chamber with a humidity probe. The same opening in the test chamber was also used to inject the iron oxide and Arizona road dust. Using the same port to measure relative humidity and inject aerosols reduces the relative humidity slightly during particle injection. However, since the injected air is only about 0.5 cfm, compared to the total flow of 15.6 cfm, the reduction in relative humidity is small.

We conducted a filter clogging and cleaning test with sub-micron iron oxide dust (Aldrich Chemical, Milwaukee, WI) to explore the possibility that sub-micron uranium oxide particles were responsible for the filter clogging. Although the average size of the uranium oxide particles was about 200  $\mu\text{m}$ , there is a significant fraction of sub-micron particles that could potentially become deeply embedded in the steel fiber medium and be difficult to remove with reverse air pulses. The density of the iron oxide particles (5.2 g/cc) is also closer to the density of the uranium oxide (11 g/cc) than the Arizona road dust (2.5 g/cc) used in most of our laboratory tests. Figure 13 shows the filter clogging and cleaning test with iron oxide aerosols on a Pall cartridge operated at 15.6 cfm and about 30% relative humidity. This test demonstrated that deposits of high density and submicron aerosols could be readily cleaned from the filter with reverse air pulses.

Any explanation of filter plugging due to particle deposits must be eliminated because it is not possible for particle deposits to cause the large decreases in pressure drop seen with the Memtec filter in Figure 11. There is no conceivable mechanism based on particle deposits that could account for large decreases in filter pressure drop by passing clean air through the filter or by letting the filter sit idle for two weeks.

We also conducted filter clogging tests under high humidity using Arizona road dust. The high humidity was generated using several spray nebulizers in a separate chamber that was connected to the inlet of the filter test apparatus. Figure 14 shows the test results from a Memtec filter cartridge during four cycles of filter clogging and cleaning at 99% relative humidity. The filter pressure drop was reduced to 4-4.5 inches after each pulse cleaning at 7 inches. Figure 15 shows a Pall filter cartridge undergoing many cycles of clogging and cleaning at 86% relative humidity. The reverse air pulse was applied when the filter pressure drop reached 15 inches. Figures 14 and 15 demonstrate that reverse air pulses can successfully clean particle deposits from the filter even under high humidity conditions. However, Figure 15 shows that, at high humidities, the pulse cleaning became less efficient over time since the resulting pressure drop after each pulse cleaning gradually increased. Comparing the clogging and cleaning cycles under high humidity in Figure 15 with that under low humidity in Figure 5 suggests that high humidity causes a gradual decay in filter cleanability. We suspect the increasing

baseline pressure drop is due to the gradual accumulation of water in the filter and not particle deposits.

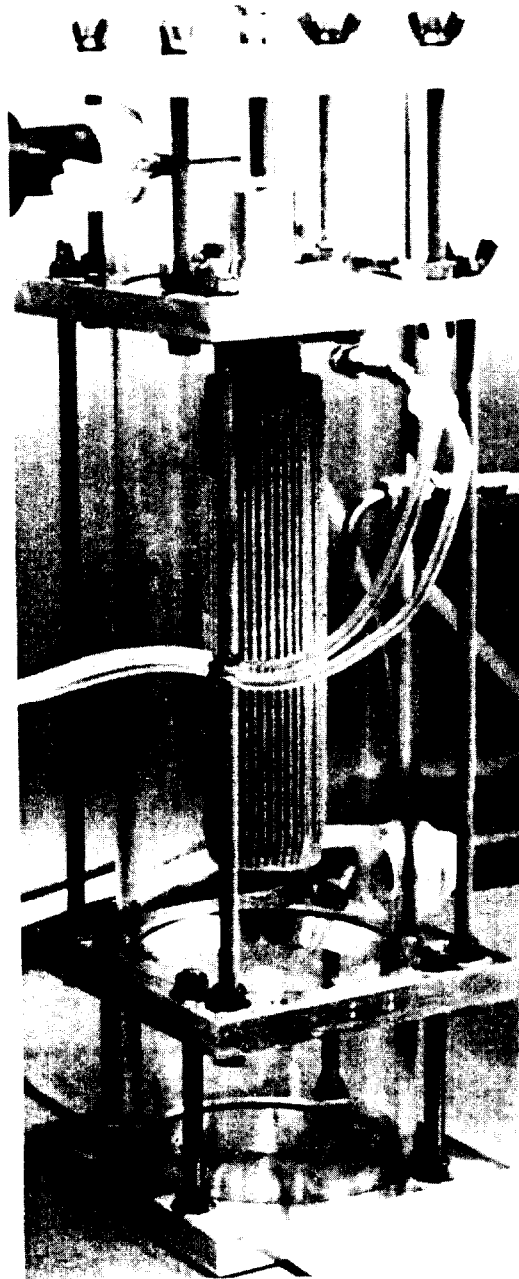


Figure 12. Filter test apparatus used for filter clogging and cleaning tests

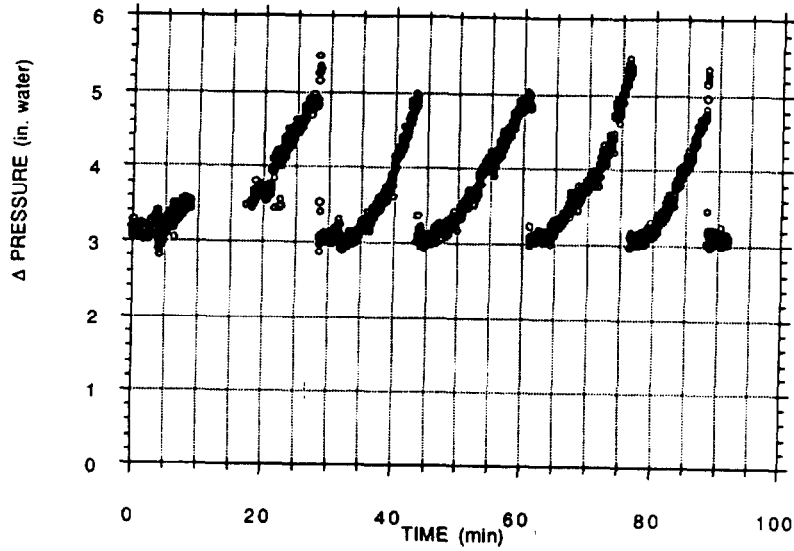


Figure 13. Filter clogging and cleaning test with submicron iron oxide dust on Pall filter cartridge at 15.6 cfm.

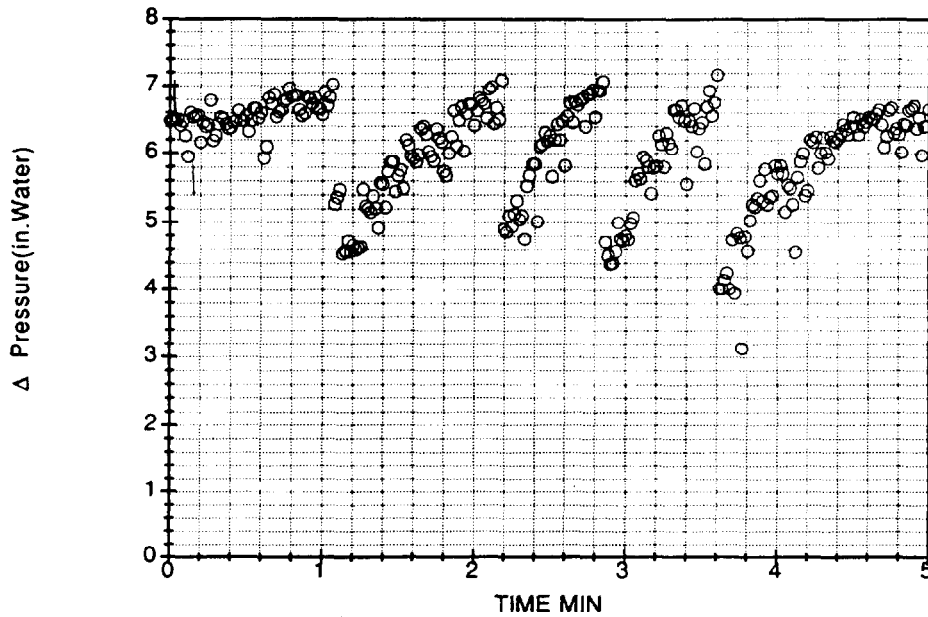


Figure 14. Filter clogging and cleaning cycles using Arizona road dust on Memtec filter cartridge at 15.6 cfm and 99% relative humidity

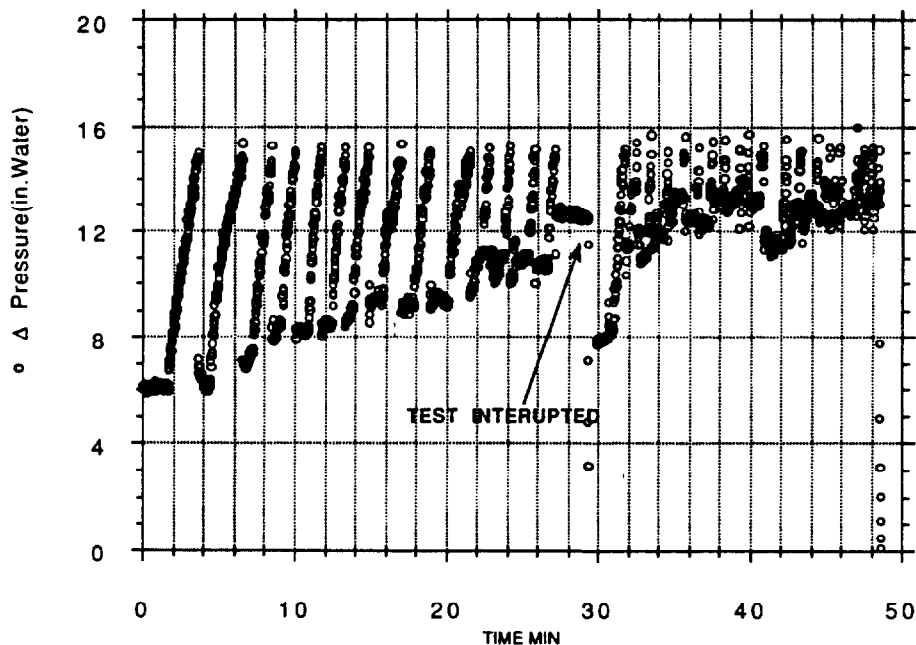


Figure 15 Filter clogging and cleaning cycles using Arizona road dust on Pall filter cartridge at 15.6 cfm and 86% relative humidity

Additional tests conducted under high humidity conditions with no aerosols confirm that the increased pressure drop and the ineffectiveness of the reverse air pulse cleaning system is due to water accumulation. Figure 16 shows the pressure drop increase as a function of time for a Pall filter cartridge when exposed to 15.6 cfm air at 100% relative humidity. The relative humidity after the filter dropped to 50%, which implies that half of the water vapor was removed by the filter. Reverse air pulses on the filter applied periodically during the water loading period had no effect on the pressure drop. The large breaks in the loading curve are due to flow adjustments required because of the increased pressure drop. The increasing pressure drop and the inability to lower it with air pulses in the laboratory tests duplicates the field observations for both the Pall filter in Figure 10 and the Memtec filter in Figure 11. The increasing pressure drop due to water accumulation is also the primary explanation for the increasing baseline pressure drop of the Pall filter being loaded with Arizona road dust at 86% relative humidity in Figure 15.

A filter clogging test using only high humidity was also conducted on a standard glass HEPA filter. Figure 17 shows the increase in pressure drop for a size 2 HEPA filter exposed to 40 cfm clean air at 100% relative humidity. Since the relative humidity downstream of the filter was 90%, only 10% of the water vapor was trapped in the filter. The large fluctuation in pressure drop in Figure 17 was due to an adjustment in the flow. Comparing the HEPA filter clogging with water in Figure 17 with the clogging seen with the grit blaster in Figure 9 suggests that water saturation may be responsible for the field clogging.

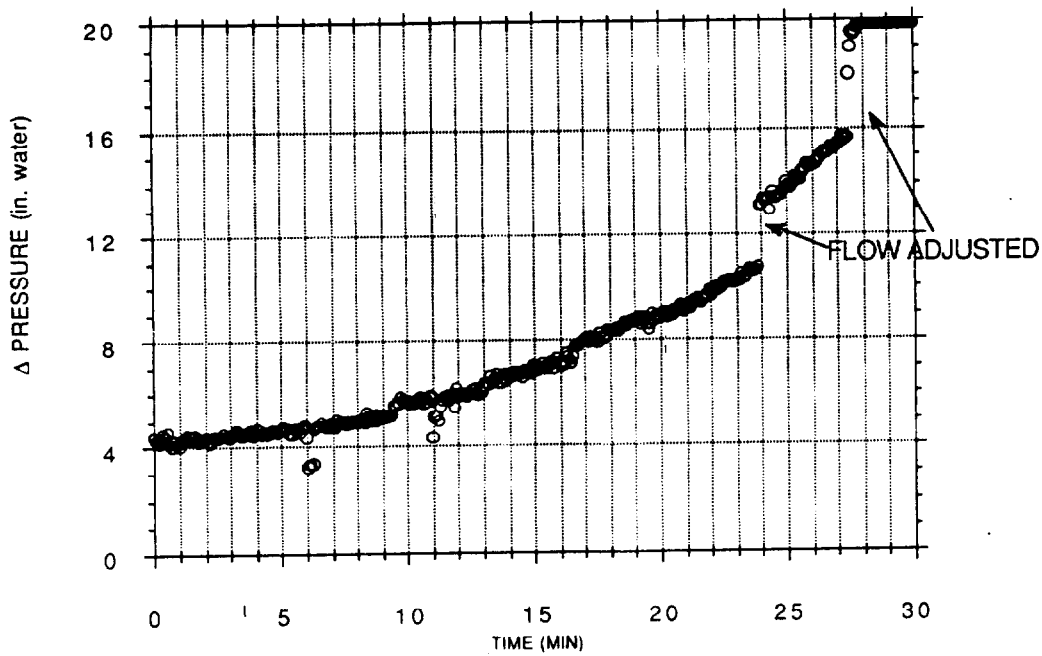


Figure 16 Filter clogging and cleaning tests with no aerosols on Pall filter cartridge at 15.6 cfm and 100% relative humidity.

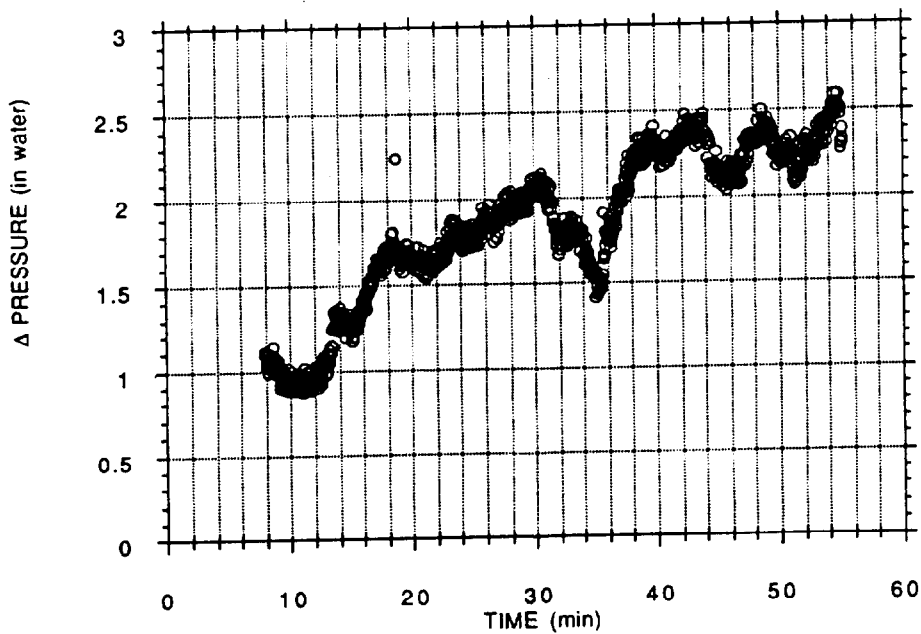


Figure 17 Filter clogging test with no aerosol on a standard glass HEPA filter at 40 cfm and 100% relative humidity

## 23rd DOE/NRC NUCLEAR AIR CLEANING AND TREATMENT CONFERENCE

Our final laboratory test was conducted to illustrate purging a steel filter saturated with water. Figure 18 shows the pressure drop, percent relative humidity, and downstream temperature of a Memtec filter that had been fully saturated with water. Purging the filter drove off the condensed water and reduced the filter pressure drop. The evaporated water raised the relative humidity to 100% and lowered the temperature of the air downstream of the filter to about 11 C. The inlet air temperature and relative humidity were 20.7 C and 36% respectively. As the amount of condensed water in the filter decreased, the pressure drop decreased. With less water available for evaporation, the temperature increased and the relative humidity decreased. Figure 18 shows that the evaporation is complete after about 120 minutes.

The laboratory purge test on the water-saturated Memtec filter in Figure 18 was able to duplicate the field observations of the Memtec filter. Figure 11 shows the pressure drop of the Memtec filter at the beginning of the field evaluation decreased from 7 inches to 4.5 inches after 14 hours of purge. The relative humidity downstream of the filter decreased from 90% to 53% during this period. The Memtec filter also showed a drop in pressure drop from 9 inches to 3 inches after sitting idle for nearly two weeks. Evaporation of condensed water in the filter is the only reasonable explanation. The large decreases in filter pressure drop in Figure 11 due to the air purge and to the two-week idle period automatically eliminate the possibility that uranium oxide particles were responsible for the observed increases in filter pressure drop.

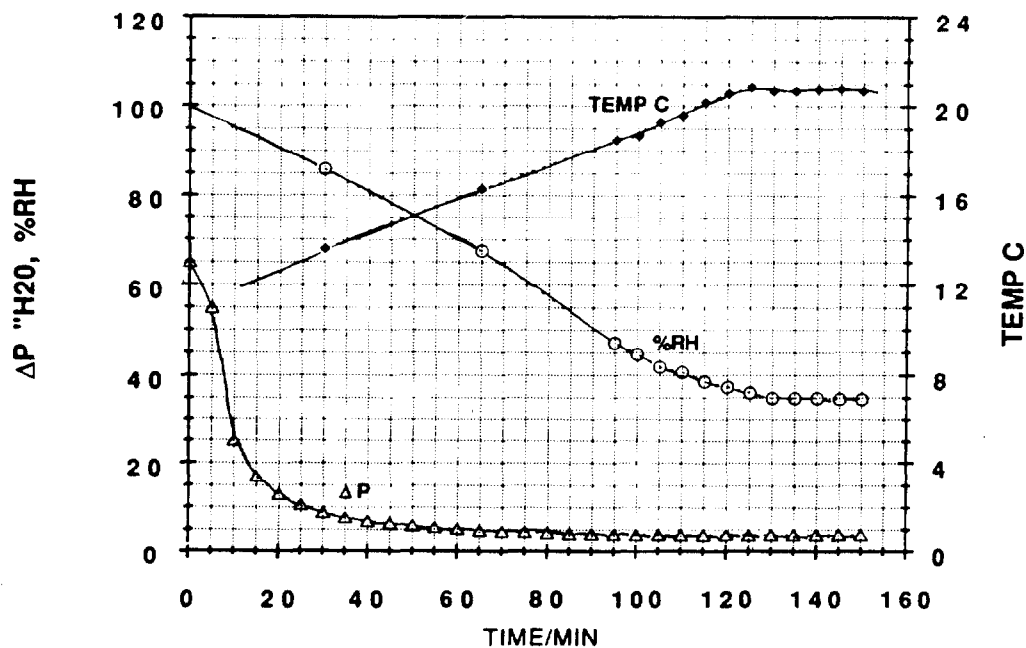


Figure 18. Purging a water-saturated Memtec filter with 15,6 cfm dry air

V. Conclusions

We have conducted a preliminary evaluation of two high efficiency steel filters in the exhaust of an uranium oxide grit blaster at the Y-12 Plant in Oak Ridge Tennessee. Test results showed both filters had a rapid increase in pressure drop with time, and reverse air pulses could not decrease the pressure drop. Subsequent laboratory tests on a single filter cartridge confirmed that water accumulation in the filter was responsible for the increase in filter pressure drop and the inability to lower the pressure drop by reverse air pulses. No effort was made to identify the source of the water accumulation and correct the problem because the available funds were exhausted.

V. Bibliography

1. Bergman, W., Connor, J., Larsen, G., Lopez, R., Turner, C., Vahla, G., Violet, C., and Williams, K., "High efficiency steel filters for nuclear air cleaning" in Proceedings of the 21st DOE/NRC Nuclear Air Cleaning Conference, CONF-90813, pp. 733-761, Feb. 1991.
2. Bergman, W., Larsen, G., Weber, F., Wilson, P., Lopez, R., Wilson, K., Moore, P., Gellner, C., Rapchun, D., Simon, K., Turley, J., Frye, L, and Monroe, D., "Development and evaluation of a cleanable high efficiency steel filter" in Proceedings of the 22nd DOE/NRC Nuclear Air Cleaning Conference, CONF-9020823, pp 586-614, July 1993.
3. "Testing of nuclear air treatment systems" Standard ASME N510-1989, American Society of Mechanical Engineers, 345 East 47th Street, New York, NY 10017.
4. "Nuclear power plant air-cleaning units and components" Standard ASME N509-1989, American Society of Mechanical Engineers, 345 East 47th Street, New York, NY 10017.
5. Simon, K., and Frye, L.E. "Demonstration and evaluation of a cleanable stainless steel high-efficiency filter" Oak Ridge Y-12 Plant Report Y/DZ-1026, June 28, 1993.



DISCUSSION

**WREN:** Have you correlated the pressure drop with the adsorbed amount of water on steel? The adsorption capacity of steel for water may not be linear but of a higher order dependence with water pressure. Thus the significant pressure drop may only be seen at high RH.

**BERGMAN:** We conducted a test at 100% relative humidity (see Figure 16) that showed water adsorption on the steel filter was responsible for a rapid increase in pressure drop. Unfortunately we did not have time to do a systematic study of water adsorption at other relative humidities.

**HULL:** Did I assume correctly that you did this in the summertime at Oak Ridge? I remember years ago when I was working down there that it certainly felt like the humidity was somewhere up around ninety percent during the summertime. Is that where the moisture came from?

**BERGMAN:** The tests were performed in April and May when there was a great deal of rain. There were heavy showers during the Pall filter evaluation.

## 23rd DOE/NRC NUCLEAR AIR CLEANING AND TREATMENT CONFERENCE

### CLOSING COMMENTS OF SESSION CO-CHAIRMAN DORMAN

We have had five papers, all dealing in some way with filters. Mr. Leonard gave his wide-ranging review of efficiency, testing, aging, quality control and so on. His paper wasn't such as to assure us that all is perfect in the filtration world. We then had two papers dealing with loading and pressure drop. Now this is a subject in which it is possible to have an infinitude of results, depending on particle size, hygroscopicity, density, shape, velocity, fiber diameter, and so on. All one can hope for in practice is to get something approaching qualitative answers and not quantitative. Nevertheless, it is highly important that we get results on this type of testing, because they help in forecasting what will happen with other types of filters; again, only qualitatively.

Figure 4 in both Mr. Dymant's and M. Vendel's paper showed rough agreement in the filter resistance vs. loading levels, up to about 300 g/m<sup>2</sup>. Both authors gave 2  $\mu$ m as the mass median diameter of the aerosol they used. I think the agreement is probably quite fortuitous, as the filters were of entirely different construction. Nevertheless, it is a point to note.

I also found it surprising in M. Vendel's Figure 4 that there was a bigger increase in pressure drop with the aerosol under dry and low humidity conditions than there was with very high humidity. I think this must be due to the hygroscopic nature of the aerosol. At high humidities, I am sure that a film is formed on the fibers, thus producing a smaller resistance rise until the liquid begins to fill the holes completely. I believe this was the thrust of one of the questioners.

The paper by Dr. Bergman suffered from the fact that he got no financial support. Nobody is rushing to give him any money at the moment, I see, but we live in hope.

The paper on magnetic filtration by Professor Watson is highly specialized. I think it is a bit out of the field in which most of us have worked. Perhaps I did not understand all the points. Perhaps some of you did. Magnetic filtration is different from other mechanisms in the fact that it is not obeying the ordinary rules of filtration, which are diffusion, interception, and inertia, and then the "stickability" of particles on the fibers. However, it is the third paper dealing with metal fibers and filters. These papers are indicative of the current interest in the performance of filters at elevated temperatures and under corrosive conditions. I foresee that for such conditions there will be a need for continuing work, and I think we shall be getting follow-up papers at the next conference.

Taken all in all, it has been quite an interesting session, with a wide variety of papers, from a general review to magnetic filters. I think Dr. Bergman's work has a future. Maybe the more we stress the finances, the more likely he is to get the money to carry on.